



BRYAN J. DOLAN  
VP, Nuclear Plant Development

Duke Energy  
EC09D / 526 South Church Street  
Charlotte, NC 28201-1006

Mailing Address:  
P.O. Box 1006 -- EC09D  
Charlotte, NC 28201-1006

704 382 0605

[bjdolan@duke-energy.com](mailto:bjdolan@duke-energy.com)

April 30, 2008

Document Control Desk  
U.S. Nuclear Regulatory Commission  
Washington, DC 20555-0001

Subject: Duke Energy Carolinas, LLC (Duke)  
William States Lee III Nuclear Station -- Docket No. 52-018  
Development of Horizontal and Vertical Site-Specific Hazard Consistent  
Uniform Hazard Response Spectra at the Lee Nuclear Station Unit 1

Reference: Dolan to NRC Document Control Desk, *Application for Combined License for William States Lee III Nuclear Station Units 1 and 2*, dated December 12, 2007.

The purpose of this letter is to provide a technical report detailing the methodology used to develop the horizontal and vertical site-specific hazard consistent uniform hazard response spectra at the William States Lee Nuclear Station Unit 1. The report is included as an enclosure to this letter.

This technical report provides a detailed presentation of analysis methodology, specifically addressing calculation approaches using random vibration theory (RVT), location-specific uniform hazard response spectra using Approach 3 (described in NUREG/CR-6728), and incorporation of site-specific aleatory and epistemic variabilities in dynamic material properties. This document supplements the analysis results presented in the Final Safety Analysis Report (FSAR), Part 2 of the referenced application.

The Unit 1 site-specific uniform hazard response spectra (UHRS) were calculated at the base of the Unit 1 nuclear island structure. As described in the FSAR, the Unit 1 foundation is supported on new and previously placed concrete materials positioned directly over continuous hard rock with shear wave velocity dominantly over 9,200 feet per second (fps). To address this configuration, location-specific UHRS were developed for the Unit 1 nuclear island. The UHRS analysis goal is to achieve site-specific response spectra which preserve the reference site hazard level and result in full site-specific hazard curves for William States Lee III Unit 1. The analyses described in the enclosed report apply to the development of horizontal and vertical uniform hazard spectra for William States Lee III Unit 1.

DOT9  
NRO

If you have any questions or need any additional information, please contact Peter Hastings, Nuclear Plant Development Licensing Manager, at (980) 373-7820.



Bryan J. Dolan  
Vice President  
Nuclear Plant Development

Enclosure:

Development of Horizontal and Vertical Site-Specific Hazard Consistent Uniform Hazard Response Spectra at the Lee Nuclear Station Unit 1

xc (w/out enclosures):

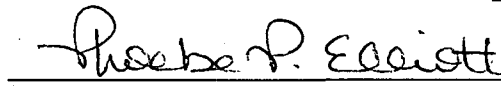
Michael Johnson, Director, Office of New Reactors  
Gary Holahan, Deputy Director, Office of New Reactors  
David Matthews, Director, Division of New Reactor Licensing  
James Lyons, Director, Site and Environmental Reviews  
Glenn Tracy, Director, Division of Construction Inspection and Operational Programs  
Luis Reyes, Regional Administrator, Region II  
Loren Plisco, Deputy Regional Administrator, Region II  
Thomas Bergmen, Deputy Division Director, DNRL  
Stephanie Coffin, Branch Chief, DNRL  
Brian Hughes, Senior Project Manager, DNRL

AFFIDAVIT OF BRYAN J. DOLAN

Bryan J. Dolan, being duly sworn, states that he is Vice President, Nuclear Plant Development, Duke Energy Carolinas, LLC, that he is authorized on the part of said Company to sign and file with the U. S. Nuclear Regulatory Commission this supplement to the combined license application for the William States Lee III Nuclear Station and that all the matter and facts set forth herein are true and correct to the best of his knowledge.

  
\_\_\_\_\_  
Bryan J. Dolan

Subscribed and sworn to me: April 30, 2008  
Date

  
\_\_\_\_\_  
Notary Public

My Commission Expires: June 26, 2011

SEAL

**ENCLOSURE No. 1**

**For**

**WILLIAM STATES LEE III NUCLEAR STATION**

**COMBINED CONSTRUCTION PERMIT AND OPERATING LICENSE COL PROJECT**

**DEVELOPMENT OF HORIZONTAL AND VERTICAL SITE-SPECIFIC HAZARD**

**CONSISTENT UNIFORM HAZARD RESPONSE SPECTRA AT**

**THE LEE NUCLEAR STATION UNIT 1**

**LEFT INTENTIONALLY BLANK**

## ACRONYMS

The definitions of acronyms used in this technical report are listed below.

1D - One Dimensional  
AEF - Annual Exceedance Frequency  
CCDF - complementary cumulative distribution function  
CENA - Central and Eastern North America  
COV - coefficient of variability  
D - distance in kilometers or miles  
EPRI - Electric Power Research Institute  
FAS - Fourier Amplitude Spectra  
FIRS - Foundation Input Response Spectra  
fps - feet per second  
FSAR - Final Safety Analysis Report  
g - acceleration unit  
GMRS - Ground Motion Response Spectra  
Hz - Hertz  
km - kilometers  
**M** - Moment Magnitude  
P - compressional wave  
PSD - Power Spectral Density  
PSHA - Probabilistic Seismic Hazard Analysis  
RMS - Root Mean Square  
RVT - Random Vibration Theory  
SDF - Single Degree of Freedom  
SV - vertically propagating shear wave  
UHRS - Uniform Hazard Response Spectra  
V/H - Vertical-to-Horizontal Ratio  
V<sub>p</sub> - compressional wave velocity  
V<sub>s</sub> - shear wave velocity  
WNA - Western North America  
km/sec - kilometers per second  
> - Greater than  
< - Less than  
≤ - Equal to or less than  
≥ - Greater than or equal to  
% - Percent

## Table of Contents

Cover Sheet.....	1
Blank Page.....	2
Acronyms.....	3
Table of Contents.....	4
List of Tables.....	4
List of Figures.....	4
REPORT OVERVIEW.....	6
1.0 INTRODUCTION.....	6
2.0 IMPLEMENTATION OF RANDOM VIBRATION THEORY (RVT) FOR SITE RESPONSE ANALYSES.....	7
2.1 RVT Durations.....	8
2.2 RVT-Based Equivalent-Linear Site-Response.....	9
3.0 APPROACHES TO DEVELOP SITE-SPECIFIC HAZARD.....	16
3.1 Description of Approaches.....	16
3.2 Approach 3 – Full Integration Method.....	19
3.3 Approach 3 – Approximate Method.....	20
3.4 Implementation of Approach.....	21
4.0 APPLICATION TO VERTICAL HAZARD.....	26
4.1 Hazard Deaggregation For The William States Lee III Nuclear Station.....	27
4.2 Development of V/H Ratios.....	27
4.3 Implementation of V/H Ratios In Developing Vertical Hazard.....	31
5.0 CONCLUSIONS.....	32
6.0 REFERENCES.....	34
7.0 TABLES AND FIGURES.....	38

## List of Tables

Cover Page.....	39
Table 1 Definitions of Locations for Motions in Site-Response Analyses.....	40
Table 2 Hard Rock Expected Horizontal Peak Acceleration Levels, Point Source Distances, and Durations.....	41
Table 3 Sample Size Required For Percent Error In The Standard Deviation For A Normal Distribution.....	42
Table 4 Moment Magnitude.....	43

## List of Figures

Cover Page.....	44
Figure 1 Comparison of median RVT and SDF (computed from acceleration time histories) 5% damped response spectra.....	45
Figure 2 Lee Nuclear Station Unit 1 amplification factors (5% damping) at a suite of Source distances.....	46
Figure 3 Example of median and $\pm 1$ sigma estimates of amplification factors computed for deep a soil site in the CENA.....	47
Figure 4 Test case illustrating the effect of magnitude on median amplification factors computed for a deep soil site in the CENA.....	49
Figure 5 Test case illustrating the effect of single-verses double-corner source spectra on median amplification factors computed for a deep soil site in the CENA.....	51
Figure 6 Test case illustrating the effect of magnitude on median amplification factors and sigma values ( $\sigma_n$ ) computed for a deep soil site in the CENA.....	53
Figure 7 Test case illustrating the effect of single-verses double-corner source spectra on median amplification factors and sigma values ( $\sigma_n$ ) computed for a deep soil site in the CENA.....	54

Figure 8 Median and sigma estimates computed for numbers of realizations from 15 to 240 using five different random seeds for a deep soil site in the CENA.....	55
Figure 9 Test case illustrating Approach 3 using a simple bilinear reference site hazard curve (dotted line, slope = 3, 6).....	56
Figure 10 Test case illustrating Approach 3 using a simple bilinear reference site hazard curve (dotted line, slope = 3, 6).....	57
Figure 11 Test case illustrating Approach 3 using a realistic (WNA) reference site hazard curve (solid line).....	58
Figure 12 Test case illustrating Approach 3 using a realistic (WNA) reference site hazard curve (solid line).....	59
Figure 13 Lee Nuclear Site hard rock horizontal hazard curve for peak acceleration (Duke Energy Carolinas, LLC, 2007).....	60
Figure 14 Lee Nuclear Station Unit 1 AEF $10^{-4}$ horizontal UHRS.....	61
Figure 15 Lee Nuclear Station Unit 1 AEF $10^{-5}$ horizontal UHRS.....	62
Figure 16 High-frequency ( $\geq 5$ Hz) and low-frequency ( $\leq 2.5$ Hz) hard rock hazard deaggregation for the Lee Nuclear Site (Duke Energy Carolinas, LLC, 2007).....	63
Figure 17 Site-specific median V/H ratios computed for the Lee Nuclear Station Unit 1 for $M$ 5.1 at a suite of distances.....	64
Figure 18 Empirical WNA soft rock median V/H ratios.....	65
Figure 19 Site-specific median and $\pm 1$ sigma V/H ratios computed for the Lee Nuclear Station Unit 1 for $M$ 5.1 at a distances of 80 km.....	66
Figure 20 Horizontal and vertical component UHRS at annual exceedance probabilities $10^{-4}$ , $10^{-5}$ , $10^{-6}$ $\text{yr}^{-1}$ .....	67



## REPORT OVERVIEW

This report presents and describes the detailed methodology used to develop horizontal and vertical hazard consistent site-specific uniform hazard response spectra (UHRS) at the Duke Energy William States Lee III Nuclear Station Unit 1. The information presented in this technical report provides a detailed presentation of analysis methodology, specifically addressing calculation approaches using random vibration theory (RVT), location-specific uniform hazard response spectra using Approach 3 (described in NUREG/CR-6728), and incorporation of site-specific aleatory and epistemic variabilities in dynamic material properties. This document supplements the analysis results presented in Section 2.5.2 of the Final Safety Analysis Report (FSAR).

The site-specific UHRS are computed as free-field motions at the ground surface, although other elevations or locations within a profile may be specified. In the case of the William States Lee III Unit 1, site-specific UHRS were calculated at the base of the Unit 1 nuclear island structure. As described in the FSAR Section 2.5.4, the William States Lee III Unit 1 foundation is supported on new and previously placed concrete materials positioned directly over continuous hard rock with shear wave velocity dominantly over 9,200 feet per second (fps). To address this configuration, location-specific UHRS were developed for the Unit 1 nuclear island. The UHRS analysis goal is to achieve site-specific response spectra which reflect the desired exceedance frequencies, or stated another way, preserve the reference site hazard level and result in full site-specific hazard curves for William States Lee III Unit 1. The analyses described in this report apply to the development of horizontal and vertical uniform hazard spectra for William States Lee III Unit 1.

## 1.0 INTRODUCTION

In developing site-specific response spectra, the usual approach involves, as a first step, a Probabilistic Seismic Hazard Analysis (PSHA) reflecting an outcropping reference site condition. The reference site condition is usually rock and, for central and eastern North America (CENA), reflects a theoretical shear-wave velocity over the top 1 km of the crust of 2.83 km/sec with a shallow crustal damping kappa value of 0.006 sec (EPRI, 1993). The shear-wave velocity is based on the empirical Mid-continent compressional-wave velocity model of Pakiser and Mooney (1989), taken by EPRI (1993) to represent the CENA, and an assumed Poisson ratio of 0.25. Since the 2.83 km/sec is but a single assigned rock shear-wave velocity, a realistic range of velocities and depths, as well as kappa values, could be developed to define a realistic range in hard rock site conditions for which hard rock attenuation relations and resulting hazard directly apply.

The kappa value, which controls high frequency motions, is empirical and based on examining motions recorded at hard rock sites (e.g. Silva and Darragh, 1995). Subsequent to the reference site condition PSHA, adjustments are made to the resulting reference site UHRS to compensate for any significant differences in dynamic material properties that may exist between the local site (Table 1) and the reference site. Table 1 describes the definitions of locations for motions in site-response analyses used in this technical report. In applying the adjustments, the goal or objective is to achieve site-specific response spectra which reflect the desired exceedance frequencies, that is, preserve the reference site annual exceedance frequency (AEF) thereby maintaining hazard consistency. The site-specific UHRS are usually computed as free-field motions at the ground surface, although other elevations or locations within a profile may be specified (Table 1).

---

\* Site condition reflected in the attenuation relations used in the PSHA

The development of horizontal and vertical hazard consistent site-specific UHRS may be considered as involving two independent analyses. The first or initial computation is the development of relative amplification factors (5% damped response spectra) between the site of interest and the reference site ( $S_a^{site}(f)/S_a^{reference}(f)$ ) that accommodates linear or nonlinear site response. Currently the state-of-practice approach involves vertically propagating shear-waves and approximations using equivalent-linear analysis using either a time domain method (e.g. SHAKE) or a more computationally efficient frequency domain random vibration theory (RVT) method.

Subsequent to the development of the amplification factors, site-specific motions are computed by scaling the reference site motions with the transfer functions. In the past, purely deterministic methods have been used but these generally result in site-specific motions that reflect higher probability than desired. More recently, semi-deterministic methods have been developed to conservatively achieve desired hazard levels, still using a fundamentally deterministic method (NUREG/CR-6728). Along with these semi-deterministic methods, fully probabilistic methods were also developed that accurately preserve the reference site hazard level and result in full site-specific hazard curves. The fully probabilistic approaches represent a viable and preferred mechanism to properly incorporate parametric aleatory and epistemic variabilities and achieve desired hazard levels and performance goals.

This report is intended to present an illustration of the two components used in the development of hazard consistent site-specific UHRS: RVT equivalent-linear site-response and fully probabilistic site-specific hazard analyses.

## **2.0 IMPLEMENTATION OF RANDOM VIBRATION THEORY (RVT) FOR SITE RESPONSE ANALYSES**

RVT reflects a classical engineering method for estimating population mean peak time domain values based on a single root mean square (RMS) estimate of the response of a system, provided the system excitation reflects stationary random noise. The advantage of using the RVT formulation is that a large number of time domain analyses are not required to obtain stable estimates of mean response. The entire response analysis can be done in the frequency domain through the use of Parseval's relation (Boore, 1983). This relation is a direct correspondence between the Fourier amplitude spectra (FAS) or power spectral density (PSD) and the time domain root-mean-square (RMS) response for any system parameter (acceleration, particle velocity, shear-strain, factor of safety against liquefaction, etc.).

The combination of RVT and Parseval's relation then permits a single linear system analysis in the frequency (power spectral) domain resulting in an estimate of time domain response that reflects a mean response over the entire population of time histories whose FAS match that of the system demand or load function. In other words, for a linear system, one which admits a frequency domain analysis and spectral superposition is appropriate (no transfer of energy between frequencies), RVT results in a peak time domain response for the entire population of phase spectra which can be associated with the PSD of the load function. In principle the load function must reflect random noise whose statistics do not vary with time (remain stationary). In applications to strong ground motions, e.g. acceleration or velocity time histories, clearly this does not appear to be the case as typical records show changes in amplitude and perhaps frequency content with time. However the randomness constraint is, fortunately, a weak constraint and extensive testing (e.g. Boore, 1983; Boore and Joyner,

1984; EPRI 1993; Silva et al., 1997; Boore, 2003) has shown the application to strong ground motion in terms of response spectra, peak acceleration, peak particle velocity, and peak shear-strains to be quite robust.

For applications to site response and strong motion, RVT is generally used in two distinct places: 1) in estimating response spectra (oscillator time domain peak values) and peak particle velocities given a ground motion FAS and duration, and 2) estimating peak shear-strain time domain values given a shear-strain FAS and duration.

## **2.1 RVT Durations**

For both applications, i.e. estimating spectral accelerations and peak particle velocities as well as peak shear-strains, durations are taken as the inverse of the source corner frequency (Boore, 1983) with a distance dependent term to accommodate the increase in duration due to wave scattering (Herrmann, 1985). For the Lee Nuclear Station Unit 1, Table 2 lists the point-source model parameters and durations used in developing site-specific V/H ratios (Section 4.2.1).

### **2.1.1 Peak-to-RMS Ratio**

Several relations exist between the time domain RMS, estimated by integrating the PSD over frequency, and the corresponding peak time domain values (Boore, 1983; 2003). These relations reflect varying degrees of approximation in the peak-to-RMS ratio, increasing in complexity and accuracy as the number of extrema over the duration decreases. Boore (1983) illustrates a range in RVT ground motion parameter estimates computed using different approximations. The maximum range is about 10% for the extreme case of only 2 extrema ( $M = 3.0$ ; Boore, 1983) over the source duration. Based on extensive comparisons of response spectra computed from time histories (referred to as single degree of freedom (SDF) spectra) with RVT estimates, Pacific Engineering typically implements an intermediate approximation. The intermediate approximation is an asymptote expression for the peak-to-RMS ratio (Equation 24; Boore, 1983) and was used in the Lee Nuclear Station Unit 1 analyses.

To integrate the PSD, numerical integration is performed rather than analytical integration, as the PSD includes site response in addition to the FAS of the simple point-source model. Because the PSD is reasonably smooth, a simple and rapid Simpson's three-point scheme is implemented but with a very dense sampling to fully accommodate the presence of peaks and troughs. Typically (e.g. Lee Nuclear Station Unit 1) 25,000 points are used from 0.007 Hz (about 150 sec) to 150 Hz. The wide integration range is to ensure inclusion of potential high- and low-frequency amplification. Additionally, the RMS is sensitive to the integration over low-frequency so it is prudent to extend its range to at-least an order of magnitude below the lowest frequency of interest, 0.1 Hz for nuclear applications (e.g. Lee Nuclear Station Unit 1). For application to other types of structures (e.g. long-span bridges, liquid natural gas facilities, etc) requiring estimates of motions to lower frequency, the integration range in FAS is extended from 0.0001 Hz to 150 Hz.

### **2.1.2 Computation of RVT Response-Spectra**

A number of procedures (equations) exist for computing response spectra (peak time domain oscillator amplitude). These equations accommodate the increasing non-stationarity of oscillatory time histories as oscillator frequency decreases. Non-stationarity becomes critical as oscillator frequency becomes lower than the source corner frequency. Under these conditions, the oscillator duration exceeds the source duration, severely violating the weak assumption of stationarity. For these cases, various correction procedures have been

developed for RVT that reflect a range in computed response spectra of about 10%. Boore (2003) gives an excellent illustration of two very different correction procedures showing their similarity for both small and large magnitude earthquake sources. For applications to transfer functions, horizontal amplification factors and vertical-to-horizontal (V/H) ratios, differences in response spectra due to different corrections at low-frequency are cancelled through taking ratios, as long as the corrections are applied consistently.

In typical Western North America (WNA) and CENA, source durations (inverse corner frequency) scale with moment magnitude ( $M$ ) such that for  $M$  5, 6, and 7, durations are approximately 1, 3, and 9 seconds respectively. As a result, corrections only become important for oscillator periods below 1, 3, or 9 seconds, depending on the magnitude used in generating the transfer functions.

Figure 1 shows an example comparison using 30 time histories from a finite fault simulation reflecting randomly selected model parameters (e.g. slip model, nucleation point, shear-wave velocity profiles etc.). Figure 1 compares median response spectra computed from time histories with RVT response spectra computed from the corresponding PSDs. In general, over the entire frequency range, the RVT spectrum agrees quite well with the SDF, reflecting a slightly smoother version. At low-frequency, the RVT spectrum is slightly above the SDF spectrum.

For the Lee Nuclear Station Unit 1, because the site response is linear and therefore magnitude independent and the maximum response is at high frequencies, the dominant source with  $M$  of 5.1 (based on deaggregations, Section 4.1) was used (Table 2). Since the maximum site response occurs at very high frequencies ( $> 50$  Hz), RVT correction procedures are not an issue. An appreciation that the correction effects are not an issue, as their impacts are cancelled in the ratios, is seen in the Unit 1 amplification factors at low frequency (Figure 2). The amplification factors remain unity down to 0.1 Hz, nearly a factor of 10 lower than the source corner frequency for an  $M$  5.1 source (Table 2). As is apparent from Figure 2, distances are not those listed in Table 2. The suite listed in Table 2 reflects the suite used for Lee Nuclear Station Unit 1 Foundation Input Response Spectra (FIRS) analyses, which included concrete fill over hard rock as well as computation of V/H ratios for Unit 1, both of which require a reasonably dense grid of reference site motions. The motivation for the distances used in Figure 2 is discussed in Section 3.4.2.3.

## 2.2 RVT-Based Equivalent-Linear Site-Response

The RVT site-response computational formulation that has been most widely employed to evaluate 1D site response assumes vertically-propagating plane shear-waves (S-waves). Departures of soil response from a linear constitutive relation are treated in an approximate manner through the use of the equivalent-linear formulation. The equivalent-linear formulation, in its present form, was introduced by Idriss and Seed (1968). A stepwise iterative analysis approach was formalized into a 1D, vertically propagating S-wave code called SHAKE (Schnabel *et al.*, 1972). Subsequently, this code has become the most widely used and validated analysis package for 1D site response calculations.

Careful validation exercises between equivalent-linear and fully nonlinear formulations using recorded motions (peak horizontal acceleration) from 0.05 to 0.5g showed little difference in results for response spectral ordinates (EPRI, 1993). Both formulations compared favorably to recorded motions suggesting both the adequacies of the vertically-propagating S-wave model and the approximate equivalent-linear formulation. While the assumptions of vertically propagating S-waves and equivalent-linear soil response represent approximations

to actual conditions, their combination has achieved demonstrated success in modeling observations of site effects and represent a stable, mature, and reliable means of estimating the effects of site conditions on strong ground motions (Schnabel *et al.*, 1972; EPRI, 1988; Schneider *et al.*, 1993; Silva *et al.*, 1997).

The vertically propagating shear-wave approach cannot successfully model amplitudes to arbitrarily long periods at deep soil sites at large source distances, as this formulation does not consider horizontally propagating surface waves. It is not clear, however, under what circumstances (profile depth, source size and distance, and structural frequency) the 1D vertically propagating shear-wave model would result in unconservative motions. Validation exercises consisting of modeling recorded motions using the 1D approximation at deep soil sites in tectonically active regions suggest the simple model performs well in terms of spectral amplitudes to periods of at least several seconds (EPRI, 1993; Silva *et al.*, 1997; Hartzell *et al.*, 1999), periods long enough to accommodate nuclear facilities.

A clear advantage of the equivalent-linear vertically propagating shear-wave model is its simplicity, resulting ease of implementation, and transparency. Due to its computational efficiency, the modeling approach is easily able to accommodate site-specific aleatory and epistemic variabilities in dynamic material properties in ground motions. This is accomplished by varying input parameters and computing the resulting motions. Unfortunately, to develop stable estimates of computed motions for each suite of parameters, multiple time histories (e.g. 5 to 15), each matched to the control motion response or Fourier amplitude spectra, must be analyzed. This is the case as peaks and troughs in response spectra as well as peak shear-strains are sensitive to the phase spectra of the control motion. For the traditional equivalent-linear formulation (e.g. SHAKE), since peak time domain shear-strains are used to iterate or soften the system (approximate nonlinear response), each time history results in somewhat different response, with the same dynamic material properties. The stacking (averaging) of responses necessary to achieve stability over multiple input time histories (all matched to the same control motion spectrum) renders the time domain (SHAKE) approach difficult to properly develop fully probabilistic response spectra.

As a practical alternative for the computation of site-response, the RVT based equivalent-linear approach (RASCALS) was developed (EPRI, 1988, 1993) and thoroughly validated (EPRI, 1993; Silva *et al.*, 1997). In this approach, which propagates an outcrop (control motion) power spectral density through a 1D soil column, RVT is used to predict peak time domain values of shear strain based upon the shear-strain power spectrum. The control motion power spectrum is propagated through the 1D rock/soil profile using the plane-wave propagators of Silva (1976). Using RVT to provide an estimate of peak time domain shear-strains results in estimates that reflect, in a single run, the mean over the entire population of control motion phase spectra, which is conditional on a single control motion power or Fourier amplitude spectrum (FAS). The computational efficiency of the RVT approach then easily allows the large number of site response analyses required to develop fully probabilistic hazard consistent response spectra as it eliminates the need for multiple time histories. For each suite of dynamic material properties, only a single site-response analysis is necessary, resulting in a mean system response over the population of phase spectra associated with the control motion PSD. Additionally, for amplification factors computed with any time domain site-response analysis procedure, the frequency-to-frequency and record-to-record variability in the computed soil response due to the time history propagation introduces additional variability. This additional variability reflects a double counting as frequency-to-frequency and record-to-record variability has already been accommodated in

the aleatory variability in the attenuation relations used in developing the reference PSHA. Employment of an RVT approach, because the control motion reflects a smooth spectrum, properly neglects the frequency-to-frequency and record-to-record variability in response spectra computed from real or realistic time histories and avoids double counting of frequency-to-frequency and record-to-record variability in the computed site response.

In the RVT implementation for peak shear-strains, the simple asymptotic expression of Equation 24 in Boore (1983) is used (Section 2.2). Based on extensive validations, this simple approach adequately reflects peak shear-strains through the soil column resulting in close comparisons between SHAKE, nonlinear codes, and recorded motions (EPRI, 1993). Careful validation exercises in modeling motions recorded from 19 earthquakes at over 500 sites quantified the accuracy of the RVT equivalent-linear approach along with the use of a point-source model to characterize control motions (EPRI, 1993; Silva et al., 1997).

### **2.2.1 Amplification Factors**

To generate amplification factors (site-specific soil  $S_a$ /reference  $S_a$ ) which properly accommodate site-specific aleatory variability, a randomization process of dynamic material properties is typically implemented about a base-case profile (EPRI, 1993). In this process, layer thickness and shear-wave velocity are randomized based on a correlation model resulting from an analysis of variance on over 500 measured shear-wave velocity profiles (EPRI, 1993). In this model, velocities are represented by a distribution at a given depth coupled to a correlation with depth, to prevent unrealistic random velocity excursions above and below a given layer. The layer thickness model is also based on measured profiles and replicates the overall observed decrease in velocity fluctuations as depth increases. This realistic trend is accommodated through increasing layer thicknesses with increasing depth. The correlation and layering model prevents unconservative profile realizations with uncorrelated velocity fluctuations over depth resulting in increased effective overall damping due to wave scattering at impedance boundaries (scattering  $\kappa$ ). This condition is exacerbated at high loading levels due to nonlinearity, concentrating shear strains in low velocity layers. As a check on this possibility it is important to compare the median response spectrum over multiple realizations with that from a single analysis with base-case properties, at low (linear) loading levels. If the median spectrum falls below that computed using the base-case dynamic material properties at high frequency by more than about 5%, a significant amount of scattering  $\kappa$  has been added in the velocity randomization, resulting in an overall larger  $\kappa$  value than desired and unconservative high-frequency motions at low loading levels. This should then be compensated by appropriately lowering the  $\kappa$  value in the control motions, another advantage of using a point-source model to generate control motions as it is not an unambiguous endeavor to adjust control motions developed from attenuation relations or spectral shapes (NUREG/CR-6728) for lower (or larger)  $\kappa$  values.

In addition to velocity and layer thickness variations, depth to basement material is also commonly randomized to cover the anticipated range over the site. For large impedance contrasts at the base of the soil, this variability smoothes the fundamental column resonance which may not be stable over multiple earthquakes (Silva et al., 1986) suggesting some degree of smoothing may be appropriate.

It is also essential to consider aleatory variability in nonlinear dynamic material properties both laterally across the site as well as vertically (where the same base-case properties are employed over a depth range). This variability in modulus reduction and damping curves is accommodated by assuming a log-normal distribution at a strain value where the curves are

changing rapidly, 0.03%, randomly sampling a distribution and applying this perturbation to the base-case curves. The perturbation is tapered approaching the ends of the curves to preserve the shape of the base-case curves. Empirical sigma values, based on laboratory test of materials of the same general type (e.g. gravely sands) such that the  $G/G_{\max}$  and hysteretic damping curves would be applied over depth ranges which boring logs or laboratory index property tests indicate appropriate, are 0.15 ( $\sigma_{\ln}$ ) and 0.30 ( $\sigma_{\ln}$ ) for modulus reduction and hysteretic damping respectively.

The  $G/G_{\max}$  and hysteretic damping curves are randomized independently. Intuitively one may expect a random excursion to a more linear modulus reduction curve would be accommodated with a higher probability of a damping curves reflecting less damping. However, such intuition may be more properly associated with mean curves rather than random excursions about mean properties. Additionally, extensive tests with negatively correlated curves showed very little difference in the variability of computed motions. This is easy to understand as hysteretic damping has a much less significant impact on computed motions than does modulus reduction. A given percentage change in  $G/G_{\max}$  results in a much larger impact on computed motions than a similar percentage change in hysteretic damping. Shear-wave velocity affects both amplification as well as energy loss through wave damping while hysteretic damping affects only energy loss. The overwhelming sensitivity of equivalent-linear site response is in the modulus reduction curves (Silva, 1992).

### 2.2.2 Control Motions

Control motions\* (PSD) may be generated by use of the single-corner (and double-corner for the CENA) point-source model reflecting the magnitude contribution to the hazard. With this approach motions are generated for reference site-conditions as well as local site-conditions by propagation from the source to the site (EPRI, 1993). Implicit in this approach is the validity of the point-source ground motion model in terms of spectral shape. Validations of the point-source model (EPRI, 1993; Silva et al., 1997; Boore, 2003) have shown the model produces realistic response spectra for a wide range in  $M$ , distance, and site-conditions. These validation exercises have demonstrated the appropriateness of the model to serve as control motions for site-response analyses and resulted in the use of the model in developing hard rock response spectral shapes and V/H ratios for the CENA (NUREG/CR-6728). A limitation of the model is its demonstrated overprediction of low-frequency response spectra at large  $M$  ( $M \geq 7.0$ ) and at close distances ( $\leq 20$  km) in the WNA (Silva et al., 1997). This observation led Atkinson and Silva (1997) to introduce a double-corner source model for large  $M$  WNA earthquakes. For the CENA, the appropriateness of the single- or double-corner source models remains an unresolved issue with most CENA attenuation relations based on the point-source model (EPRI, 2004). For reference site conditions consisting of hard rock in the CENA, the single- and double-corner source model spectral shapes presented in NUREG/CR-6728 may also be used as control motions. Uncertainty in single- versus double-corner models results in the recommendation of computation of amplification factors using both models and combining the resulting hazard curves with the same relative weights as used in developing the reference (e.g. hard rock) PSHA.

For applications to the WNA, rock control motions may be generated using empirical attenuation relations or spectral shapes presented in NUREG/CR-6728, after adjusting the surface outcrop motions to base-of-soil conditions (NUREG/CR-6728). Alternatively, the

---

\* Control Motion: Motion used as input to site response analyses. This can be reflected in time histories matched or scaled to a response spectrum or, in the case of RVT, a PSD.

point-source single-corner frequency model may be used with  $M$  limited to about  $M$  7.0 for deep soil sites to avoid overdriving the soil column at low-frequency ( $< 1$  Hz). Alternatively or in conjunction, the WNA double-corner source model (Atkinson and Silva, 1997) may be used as control motions. Use of the point-source models reflects computational efficiency as it avoids the intermediate step of spectral matching to the empirical spectra, which are not well constrained for all  $M$  at distances exceeding about 100 km.

#### **2.2.2.1 Effects of Spectral Shape**

In the development of amplification factors, the shape of the control motion spectrum plays an important role due to nonlinearity in the site-response. The three factors which control spectral shape, apart from site effects include: magnitude (through the source corner frequency), single- versus double-corner source spectra, and distance (through depletion of high-frequency energy as distance increases) (Silva et al., 1997). In principle all three dependencies in control motion spectral shape should be accommodated in developing amplification factors. Accommodating these potential dependencies on control motion spectral shape would result in development of hundreds of mean amplification factors at a fine discrete grid of values for  $M$ , e.g. every 0.1 unit in  $M$ , and in distance, e.g. every 1 to 2 km in distance over the ranges of contributions to the reference hazard. For the CENA, separate suites of amplification factors computed for both single- and double-corner source models would be required as well. However, the actual dependencies have been examined through sensitivity analyses, resulting in general guidelines in magnitude and distance dependencies that produce significant ( $\geq 10\%$ ) differences in mean amplification factors.

For deterministic approaches in developing site-specific UHS (Section 3.1, Approaches 1 and 2), typically only two magnitudes and associated distances are used reflecting the high-frequency (5 Hz to 10 Hz, 5 Hz and above) and low-frequency (1 Hz to 2.5 Hz, 2.5 Hz and below) contributions to the reference hazard (NUREG/CR-6728). However, for the fully probabilistic approach to developing site-specific UHS (Section 3.1, Approach 3), a wide range in levels of reference site spectra is required as the entire reference (e.g. hard rock) hazard curve has contributions to each point (exceedance frequency) on the site-specific (e.g. soil) hazard curve. Typically the range in levels of reference site spectra is accommodated through a suite of expected reference site peak acceleration values, conditional on  $M$ , generated by varying source distances (Table 2). This approach then naturally accommodates any dependence on distance in the amplification factors due to the effects of distance on control motion spectral shape.

To illustrate effects of control motion loading level on amplification factors, Figure 3 shows median and  $\pm 1$  sigma estimates computed for a generic deep soil site in the CENA using a single-corner frequency  $M$  7.0 point source model. Reference (hard rock, Table 2) expected peak accelerations range from 0.01g to 1.50g at 11 discrete values with distances ranging from about 300 km to 0 km (several km depth). As Figure 3 clearly shows, at frequencies exceeding about 2 Hz, amplification decreases as loading levels increase. Also apparent, at high frequency, is the increase in sigma with increasing loading levels. This is due to the inclusion of aleatory variability through the randomization of modulus reduction and hysteretic damping curves. As loading levels increase, nonlinearity becomes more important, appropriately reflecting a larger total aleatory variability. Also apparent in Figure 3 is the large deamplification at very high loading levels reaching a minimum for the median at about 30 Hz near 0.2. Based on empirical attenuation relations (e.g. Abrahamson and Shedlock, 1997), the minimum for observations available through 1997 is about 0.5. The

---

\* Median estimates



minimum value shown in Figure 3 of about 0.2 may be a result of the equivalent-linear approximation, using a single value of shear-wave velocity and damping at all frequencies. As a result, a minimum amplification of 0.5 is implemented, based on observations.

To illustrate the effect of magnitude on amplification factors, Figure 4 shows median amplification factors computed for **M** 5, 6, and 7 for the same generic profile using single-corner-frequency point-source models. At low levels of motion, 0.01g to 0.10g, there is a strong **M** dependency at high-frequency ( $\geq 20$  Hz). This is principally due to distance effects, depleting the larger **M** high-frequency control motion. This observation is due to the increased width of the oscillator transfer function as oscillator frequency increases. At the large distances for **M** 6 and **M** 7 (beyond 200 km and 300 km respectively), the Fourier amplitude spectrum is severely depleted. As a result, the high-frequency oscillators reach back to low-frequency for energy such that the amplification factors reflect lower frequency values. This is precisely the same phenomenon which causes response spectral acceleration to saturate to peak acceleration at high frequency. While these **M** dependencies due to distance are quite large at high-frequency, they become insignificant at frequencies of interest ( $\leq 30$  Hz) for loading levels of concern (above 10%g). This observation also points out a possible limitation of the CENA spectral shapes in NUREG/CR-6728. For consistency with the empirical WNA shapes, the CENA shapes were defined only to a distance of 200 km. Use of these shapes for larger distances will likely result in too much high-frequency energy and unconservative amplification factors at low levels of motions and at high-frequency. For the case of the Lee Nuclear Station Unit 1, the similarity of the amplifications, median and sigma estimates, over the distance range of 1 km to 200 km (Figure 2) indicates this observation is not an issue. This is the case as the fundamental resonance for the Lee Nuclear Station Unit 1 is near 90 Hz (Section 3.4.2.3), well beyond the peak in the hard rock spectral shapes (NUREG/CR-6728). As a result, even at a distance of 1 km, the Fourier amplitude spectrum is depleted.

Of significance for the development of UHRS for nuclear facilities is the range in median amplification over the 1 Hz to 20 Hz range for **M** 5, 6, and 7 shown in Figure 4. In general, for loading levels up to about 0.75g, which covers the range of interest for AEF of  $10^{-4}$  and  $10^{-5}$  over most of the CENA, the range in amplification is about 20% for a unit change in magnitude. Based on sensitivity analyses such as these as well as the observation of Bazzurro and Cornell (2004) of an even weaker magnitude dependency, from analyses with recorded motions, a conservative guideline for accommodation of magnitude dependencies in the reference hazard deaggregation is about one half magnitude unit. That is, one should maintain the model magnitudes as a function of structural as well as exceedance frequency from the reference deaggregation to a precision of about one half magnitude unit. This approximation recognizes both the magnitude dependency of amplification factors as well as the range in magnitudes contributing to the reference hazard at a given structural and exceedance frequency. Use of the mode is clearly more appropriate than the mean, even though there is rarely a single peak over magnitude.

These results point out the inappropriateness of simply scaling control motions up and down to reflect either different magnitude sources or different distances, conditional on magnitude.

To illustrate the potential effects of source processes in the CENA in terms of single- versus double-corner source spectra, Figure 5 shows a comparison of median amplification factors computed for the same suite of expected horizontal hard rock (reference) peak acceleration values. As with the magnitude dependencies shown in the low loading levels in Figure 4, the differences between the amplification factors computed with the two source models at

0.01g are, in reality, due to differences in distances (317 km and 340 km for the single- and double-corner source models respectively). Of more relevance and significance are the differences in median amplification factors at higher loading levels ( $\geq 0.20g$ ) in the 1 Hz to 20 Hz frequency range. In this frequency range, the differences steadily increase from about 5% to 10% at 0.2g to over 20% at 0.75g with the amplification factors computed with the two-corner model exceeding those computed with the single-corner source model. The converse is true below the fundamental column resonance near 0.2 Hz. These trends are a result of lower intermediate frequency source spectra for the double-corner source model compared to the single-corner model (NUREG/CR-6728). This results in lower loading levels, more linear response, for the double-corner source model, leading to larger intermediate frequency amplification and less of a shift the fundamental column resonance to lower frequency. It is important to point out this effect would be greater for larger magnitudes as well as less for smaller magnitudes, becoming insignificant for magnitude less than about 5.25. This can be appreciated by comparing response spectral shapes illustrated in NUREG/CR-6728 as the spectral sag of the double-corner source model largely disappears at **M** 5.0.

To provide a further illustration of the impacts of magnitude and source processes on median amplification factors as well as their associated aleatory variabilities, Figures 6 and 7 show results plotted versus reference (hard rock) response spectra for selected frequencies (100 Hz, 10 Hz, and 1.0 Hz). These plots display the factors and standard deviations in the manner of which they are implemented in the fully probabilistic approach to developing site-specific UHRS (Section 3.0). Figure 6 shows the effects of control motion magnitude on median amplification factors and their aleatory variabilities conditional on the reference spectral acceleration. The range in loading level (0.01g to 1.50g) is seen in the frame for 100 Hz (peak acceleration by definition). The corresponding ranges in 10 Hz and 1 Hz hard rock response spectra are displayed in the corresponding frames. Figure 6 illustrates the smooth nature of the factors and their aleatory variabilities as well as the clear magnitude and loading level dependencies. The overall smoothness of the amplification factors and standard deviations is significant as linear (log scale) interpolation is used to develop estimates between the discrete loading levels (e.g. Table 2).

As previously mentioned, the positive slope of the sigma values reflects the important impact of the aleatory variability in the randomization of the  $G/G_{max}$  and hysteretic damping curves. As loading level increases, nonlinear dynamic material properties exert more of an influence (become more important) on computed motions. As expected, peak acceleration has the lowest variability. Empirically, peak acceleration is the most stable and therefore most accurately known strong ground motion parameter (Abrahamson and Shedlock, 1997). The decrease in variability with increasing magnitude and increasing loading level is also expected. Larger magnitude sources are statistically stable (stationary) for longer durations and, as loading level increases, nonlinearity tends to buffer or reduce fluctuations or variability in response. At low levels of loading, doubling control motions may double soil peak acceleration while at high loading levels, due to nonlinearity, doubling control motions increases soil motions by a smaller degree.

Completing the illustration, Figure 7 shows a similar comparison between single- and double-corner source models for **M** 7.0. As with Figure 6, similar trends are shown for the double-corner source model, smooth variation of median amplification and aleatory variability with variations in loading levels.

Alternatively, in lieu of the point-source model, the spectral shapes (NUREG/CR-6728) may be used as hard (CENA, single- and double-corner) rock or soft (WNA) rock (adjusted for base-of-soil conditions, NUREG/CR-6728) control motions. For use in the RVT equivalent-linear analyses, an RVT spectral match is performed generating a FAS whose RVT response spectrum matches the target or appropriate spectral shape (NUREG/CR-6728). As another alternative for control motions, the attenuation relations used in developing the reference PSHA may be used, provided the reference site condition is rock and for soft outcropping rock, the resulting rock spectra are adjusted for base-of-soil conditions (NUREG/CR-6728). With this approach, separate amplification factors should be developed using spectra computed for each attenuation relation as control motions to accommodate potential epistemic variability in site-response due to the differences in spectral shape among the attenuation relations. The resulting amplification factors should then be combined with the same relative weights as used in developing the reference PSHA. Additionally, for the CENA, amplification factors computed for the single- and double-corner source models should be combined with the same relative weights as used in developing the reference PSHA.

### 3.0 APPROACHES TO DEVELOP SITE-SPECIFIC HAZARD

In developing site-specific UHRS or hazard there are two goals which must be met to achieve desired risk levels:

- 1) Preserve the hazard level (AEF) of the reference site PSHA across structural frequency to achieve hazard consistency and,
- 2) Incorporate site-specific aleatory (randomness) and epistemic (uncertainty) variabilities of dynamic material properties in the hazard.

#### 3.1 Description of Approaches

In general, there are four fairly distinct approaches intended to accomplish the stated goals. The approaches range from the simplest and least accurate (Approach 1), which scales the reference site UHRS on the basis of a site-response analysis using a broad-band control motion to the most complex and most accurate, a PSHA computed using attenuation relations, median estimates and standard deviations, developed for the specific-site (Approach 4).

**Approach 1:** This approach is fundamentally deterministic and involves, for a rock reference site, use of the outcrop UHRS to drive the site-specific column(s). By definition it assumes a rock outcrop UHRS has similar characteristics as rock beneath soil, not generally a valid assumption for soft rock (NUREG/CR-6728), and has no mechanism to conserve the outcrop AEF. For cases where the hazard is dominated by earthquakes with significantly different  $M$  at low (e.g.  $\leq 1$  Hz to 2.5 Hz) and high (e.g.  $\geq 5$  Hz to 10 Hz) structural frequencies, the outcrop UHRS may be quite broad, unlike any single earthquake, resulting in unconservative high-frequency motions (too nonlinear in site response). Even if only a single earthquake is the major contributor at all structural frequencies, variabilities incorporated in the hazard analysis may result in a broad spectrum, again unlike any single earthquake. For these reasons, this approach is discouraged and Approach 2, an alternative semi-deterministic method may be used.

**Approach 2:** This approach is also fundamentally deterministic and is intended to avoid the broad-band control motion of Approach 1. For a rock reference site, Approach 2 uses low- and high-frequency (and intermediate if necessary) deterministic spectra computed from the

attenuation relations used in the PSHA, or suitable spectral shapes (NUREG/CR-6728) reflecting expected rock conditions beneath the local soils, scaled to the UHRS at the appropriate frequencies (e.g., RG 1.165). These scaled motions, computed for the modal deaggregation  $M$  and  $D$  are then used as control motions to develop multiple (typically 2 to 3) mean transfer functions based on randomized soil columns. If the control motions are developed from the attenuation relations used in the reference PSHA, the generic site condition they reflect must be appropriate for the rock beneath the local soils. Additionally, separate control motions should be developed for each attenuation relation to include the effects of spectral shape uncertainty (epistemic) on soil response. The resulting mean transfer functions would then be combined using the same relative weights as in the reference PSHA. The mean transfer functions are then enveloped with the resulting transfer function applied to the outcrop (rock or soil) UHRS. This method was termed Approach 2A in NUREG/CR-6728. The use of mean (rather than median) transfer functions followed by enveloping is an empirical procedure to conservatively maintain the outcrop exceedance probability (NUREG/CR-6728 and - 6769), as this fundamentally deterministic approach does not include the contributions to soil spectra from the entire range in rock or reference site hazard (Bazzurro and Cornell, 2004). The motivation for this "empirical" procedure is discussed in Section 3.3 (Approach 3 – Approximate Method).

For cases where there may be a wide magnitude range contributing to the hazard at low- or high-frequency and/or the site has highly nonlinear dynamic material properties, low, medium, and high  $M$  control motion spectra may be developed at each frequency of interest. A weighted mean transfer function (e.g., with weight of 0.2, 0.6, 0.2 reflecting 5%, mean, 95%  $M$  contributions) is then developed at each structural frequency of interest. Following Approach 2A, the weighted mean transfer functions for each frequency of interest are then enveloped with the resultant applied to the outcrop UHRS. This more detailed analysis procedure was termed Approach 2B in NUREG/CR-6728.

**Approach 3:** This approach is a fully probabilistic analysis procedure, which moves the site response, in an approximate way, into the hazard integral. The approach is described by Bazzurro and Cornell (2004) and NUREG/CR-6769. In this approach, the hazard at the soil surface is computed by integrating the site-specific hazard curve at the bedrock level with the probability distribution of the amplification factors (Lee *et al.*, 1998; 1999). The site-specific amplification, relative to CENA rock (in the case of the Lee Nuclear Station Unit 1), is characterized by a suite of frequency-dependent amplification factors that can account for nonlinearity in soil response. Approach 3 involves approximations to the hazard integration using suites of transfer functions, which result in complete hazard curves at the ground surface, or any other location, for specific ground motion parameters (e.g., spectral accelerations) and a range of frequencies.

The basis for Approach 3 is a modification of the standard PSHA integration:

$$P[A_S > z] = \iiint P \left[ AF > \frac{z}{a} \mid m, r, a \right] f_{M,R|A}(m, r; a) f_A(a) dm dr da \quad (1)$$

where  $A_S$  is the random ground motion amplitude on soil at a certain natural frequency,  $z$  is a specific level of  $A_S$ ,  $m$  is earthquake magnitude,  $r$  is distance,  $a$  is an amplitude level of the random reference site (e.g. hard rock) ground motion,  $A$ , at the same frequency as  $A_S$ ,  $f_A(a)$  is derived from the rock hazard curve for this frequency (namely it is the absolute value of its

derivative), and  $f_{M,R|A}$  is the deaggregated hazard (i.e., the joint distribution of M and R, given that the rock amplitude is level a). AF is an amplification factor defined as:

$$AF = A_s/a \quad (2)$$

where AF is a random variable with a distribution that can be a function of m, r, and a. To accommodate epistemic uncertainties in site dynamic material properties, multiple suites of AF may be used and the resulting hazard curves combined with weights to properly reflect mean hazard and fractiles.

Soil response, in terms of site amplification ( $S_a$  (site)/ $S_a$  (reference)), is controlled primarily by the amplitude of rock motion and m, so Equation 1 can be approximated by:

$$P[A_s > z] = \iint P[AF > \frac{z}{a} | m, a] f_{M|A}(m; a) f_A(a) dm da \quad (3)$$

where r is dropped because it has an insignificant effect in most applications. To implement Equation 3, only the conditional magnitude distribution for relevant amplitudes of a is needed.  $f_{M|A}(m; a)$  can be represented (with successively less accuracy) by a continuous function, with three discrete values or with a single point, (e.g.,  $m^1(a)$ , the model magnitude given a). With the latter, Equation 3 can be simplified to:

$$P[A_s > z] = \int P[AF > \frac{z}{a} | a, m^1(a)] f_A(a) da \quad (4)$$

where,  $f_{M|A}(m; a)$  has been replaced with  $m^1$  derived from deaggregation. With this equation, one can integrate over the rock acceleration, a, to calculate  $P[A_s > z]$  for a range of soil amplitudes, z.

It is important to note there are two ways to implement Approach 3: the full integration method described below, or by simply modifying the attenuation relation ground motion value during the hazard analysis with a suite of transfer functions (Cramer, 2003). Both implementations result in very similar site-specific hazards (Cramer, 2003) and both will tend to double count site aleatory variability, once in the suite of transfer function realizations and again in the aleatory variability about each median attenuation relation. The full integration method tends to lessen any potential impacts of the large total site aleatory variability (Bazzurro and Cornell, 2004). Approximate corrections for the site component of aleatory variability, may be made by implementing the approximate technique (Equation 7, Section 3.3) with  $C = 0$ ,  $AF = 1$ , and a negative exponential, where  $a_{rp}$  = the soil amplitude and  $\sigma$  the component of variability that is removed. For the typical aleatory variability of the amplification factors ( $\sigma_{ln} \approx 0.1-0.3$  e.g. Figures 5 and 6) and typical hazard curve slopes in the CENA ( $\kappa \approx 2-3$ , Figure 13), the reduction in motion is about 5% to 10%.

**Approach 4:** Approach 4 entails the development and use of site-specific attenuation relationships, median estimates, and aleatory variabilities, developed specifically for the site of interest which incorporate the site response characteristics of the site. The PSHA is performed using these site-specific relationships for the specified AEF. This approach is considered the most accurate as it is intended to accommodate the appropriate amounts of aleatory variability into site and region specific attenuation relations. Epistemic variability is

appropriately captured through the use of multiple attenuation relations. Approach 3 is considered a fully probabilistic approximation to Approach 4.

### 3.2 Approach 3 – Full Integration Method

The site-specific hazard curve can be calculated using the discretized form of Equation 3 from Bazzurro and Cornell (2004).

$$G_z(z) = \sum_{\text{all } x_j} P\left[Y \geq \frac{z}{x} \middle| x_j\right] p_X(x_j) = \sum_{\text{all } x_j} G_{Y|X}\left(\frac{z}{x} \middle| x_j\right) p_X(x_j) \quad (5)$$

where  $G_z(z)$  is the sought hazard curve for  $S_a^s(f)$ , that is, the annual probability of exceeding level  $z$ .

$$G_{Y|X}\left(\frac{z}{x} \middle| x\right) = \hat{O} \left( \frac{\ln\left[\frac{z}{x}\right] - \ln\left[\hat{m}_{Y|X}(x)\right]}{\sigma_{\ln Y|X}} \right) \quad (6)$$

where  $G_{Y|X}$  is the complementary cumulative distribution function of (CCDF)  $Y = AF(f)$ , conditional on a rock amplitude  $x$ . This is simply the CCDF of the site amplification factors as a function of control motion (e.g. rock or reference site) loading level.

$\hat{O} = 1 - \bar{O}$  - the widely tabulated complementary standard Gaussian cumulative distribution function.

$\hat{m}_{Y|X}$  - the conditional median of  $Y$  (the amplification factor).

$\sigma_{\ln Y|X}$  - the conditional standard deviation of the natural logarithm of  $Y$  (aleatory variability of the amplification factor).

$p_X(x_j)$  - the probability that the rock or reference site control motion level is equal to (or better, in the neighborhood of)  $x_j$ .

Equation 5 is the essence of Approach 3 and simply states that the soil hazard curve is computed as the product of the soil amplification (specifically its CCDF), conditional on a reference (rock) amplitude  $x$ , times the probability of obtaining that reference amplitude, summed over all reference amplitudes.

The soil amplifications, median and  $\sigma_{\ln}$  estimates are all that are required, and are generated by driving the soil column with a suite of reference site motions (Section 2.2). At each reference motion, multiple realizations of randomized dynamic material properties are developed followed by site response analyses to generate a suite, typically 30 to 100 (Section 3.4.1), of amplification factors. From that suite, a median and  $\sigma_{\ln}$  is computed, generally assuming a log-normal distribution.

The probability of obtaining a reference motion is the derivative of the reference (e.g. rock) hazard curve obtained from the PSHA. This is done numerically and is a stable process as

the hazard curves are quite smooth. Equation 5 can quite easily be entered into an EXCEL spread sheet. Approach 3 is indeed, one simple equation.

### 3.3 Approach 3 – Approximate Method

An alternative solution to Equation 4 can also be calculated using Equation (7) from Bazzurro and Cornell (2004). This is a closed form approximation of the integration of the amplification factor over a range of rock amplitudes.

$$z_{rp} = a_{rp} \overline{AF}_{rp} \exp\left(\frac{\sigma_{\delta}^2}{2} \frac{\kappa}{1-C}\right) \quad (7)$$

where  $z_{rp}$  is soil amplitude  $z$  associated with return period  $r_p$ ;  $a_{rp}$  is the reference spectral acceleration  $a$  associated with return period  $r_p$ ;  $\overline{AF}_{rp}$  is the geometric mean (mean log) amplification factor for the reference (e.g. rock) motions with return period  $r_p$ ;  $\kappa$  is the log-log slope of the reference hazard curve that is calculated at each point from the reference hazard curve and ranges from about 2 to 3 for CENA and possibly as large as 6 for WNA.  $C$  is the log-log slope (absolute value) of the amplification factor with respect to the reference motion that is calculated at each point from the amplification factors, AF and is a measure of the degree of soil nonlinearity. If  $C = 0$ , the response is linear and highly nonlinear for  $C$  approaching 1, where the approximation breaks down (Bazzurro and Cornell, 2004). As previously mentioned,  $C$  ranges from about 0.1 to about 0.8 (Bazzurro and Cornell, 2004).  $\sigma_{\delta}$  is the log standard deviation of the AF and is around 0.3 ( $\sigma_{ln}$ ) or less (Figures 6 and 7). In other words, at a given AEF or point on the reference site hazard curve, the corresponding soil amplitude is given as the median soil amplification times the rock or reference site amplitude plus an exponential factor.

The exponential factor is necessary to maintain the reference AEF and accommodates both the aleatory variability as well as the degree of nonlinearity of the site amplification. The slope of the reference hazard curve is a weighting factor that includes the contributions to the soil amplitude for all reference hazard levels. Equation 7 clearly demonstrates the additional factors needed over median amplification to preserve the hazard level (AEF) of the reference motion. This Equation shows that in order to preserve the reference site (e.g. rock) hazard level, multiplying the reference motion by the median soil amplification requires an additional exponential term. This additional term includes the aleatory variability of the soil or amplification factor, the slope of the reference site hazard curve, as well as the slope of the amplification factors (e.g. with varying reference motion). This exponential factor accommodates the potential contributions to a given soil motion by the entire range in reference site motions due to soil nonlinearity. That is, a given soil motion may have the same value at low levels of reference loading (relatively linear response) and at high loading levels (relatively nonlinear response). To preserve the reference site exceedance frequency, all the contributions to a given soil motions over the entire range in reference loading levels must be included in the soil hazard. These contributions are not explicitly considered in the deterministic Approach 2 method. Additionally, the effects of aleatory variability in the soil amplification due to lateral variability in velocities and depth to basement as well as randomness in  $G/G_{max}$  and hysteretic damping curves are included in the exponential term. For a linear site,  $C$  is zero so it is easy to see the exponential term then accommodates the effects of profile variability in the soil hazard. The reference hazard curve slope ( $\kappa$  in Equation 7) is present to accommodate the impacts of the soil variability and nonlinear amplification over the entire reference site motion or hazard curve. In the

case  $C = 0$  and for a reference hazard slope near 1, the median amplification times the exponential term simply reflects the mean, for a lognormal distribution. This was the motivation for using mean, rather than median amplification factors in Approach 2. However, for more realistic reference site hazard curve slopes, use of the mean amplification alone will result in motions that are too low for the assumed AEF. The difference or underestimation increases as soil nonlinearity, characterized through  $C$ , becomes larger for a given aleatory variability in the amplification factors. This was the motivation for the "empirical" correction in Approach 2 of enveloping the low- and high-frequency transfer functions. The high-frequency transfer function will typically have lower high-frequency amplification than the low-frequency amplification factor as it reflects higher loading levels, resulting in a higher degree of nonlinearity, and a greater value of  $C$ . Use of mean amplification alone may then depart significantly from Equation 7 resulting in higher probability motions than would be consistent with the reference hazard level, depending on the value of  $C$  and the slope of the reference hazard curve. Using an envelope of the low-frequency amplification, which typically does not reflect nearly as high loading levels at high-frequency, and the high-frequency amplification was an ad-hoc manner of conservatively achieving the desired AEF using deterministic analyses.

It is important to point out that a similar issue, though less significant, can occur at low-frequency. In this case the high-frequency amplification has larger low-frequency amplification than the low-frequency amplification. The envelope at low-frequency is then controlled by the high-frequency amplification, compensating for the neglect of the complete exponential in the low-frequency mean amplification (NUREG/CR-6728).

### 3.4 Implementation of Approach 3

Approach 3 is implemented using the full integration method which consists simply of coding Equation 5. The soil (or rock) amplification distributions relative to the reference site condition are developed by driving the site-specific column at a suite of distances generated on a grid of expected reference site peak accelerations (Table 2), to accommodate nonlinear soil response. At each distance, or reference site expected peak acceleration, random suites of dynamic material properties are generated resulting in a distribution of structural frequency dependent amplification factors ( $S_a(\text{site})/S_a(\text{reference})$ ). For a given structural frequency (e.g. 1 Hz), this process results in median and sigma estimates, for each loading level, from which a CCDF is produced using standard asymptotic expressions, typically accurate to the fourth decimal place. For each loading level, reference  $S_a$  at 1 Hz, the amplification CCDF is then available to integrate over the entire reference 1 Hz hazard curve. This is precisely the motivation for the wide range in reference peak accelerations, 0.01g to 1.50g (Table 2), to cover the entire reference hazard curve for each structural frequency. For reference site motion outside the range, the closest values are used. To minimize any error in interpolation (log) for reference site motions between grid points (Table 2), a dense sampling of typically 11 values of expected reference site peak accelerations is used. The array of peak accelerations is sampled more densely over the range in values contributing most to the hazard, usually 0.2g to 0.5g. Since the amplification factors are smooth (e.g. Figures 6 and 7 and Bazzurro and Cornell, 2004; Silva et al., 1999), interpolation is not a significant issue and the 11 point grid listed in Table 2 is adequate to capture site nonlinearity.

To compute the probability of reference motions ( $P(x)$  in Equation 5), the reference motion hazard curve is numerically differentiated using central differences. Although hazard curves are smooth so differencing is a stable process, the curves are interpolated to 100 points to



maximize the integration accuracy of Equation 5. The use of 100 points was established by increasing the number of points until stability (no change in derived soil hazard) was achieved to an AEF of about  $10^{-10}$ . Using this approach, stability usually occurred at about 50 points so 100 points has been adopted as a conservative value for integration.

It is important to point out that because multiple levels of reference motions contribute to the soil or site-specific hazard, a wider range in reference hazard than soil hazard is necessary to achieve accuracy in the soil hazard. Extensive tests have shown that a conservative range over which to integrate the reference hazard is a factor of 10 in AEF beyond that desired for the soil or site-specific AEF. In other words, if site-specific hazard is desired to  $10^{-6}$  AEF, reference hazard is required to an AEF of  $10^{-7}$ . Additionally, the same consideration applies at high exceedance frequencies as well. In this case, if site-specific hazard is desired at  $10^{-2}$  AEF, reference hazard is conservatively required to an AEF of  $10^{-1}$ .

Approach 3 is also appropriate for computing site-specific vertical hazard from horizontal site-specific hazard curves, producing vertical UHRS at the same AEF as the horizontal UHRS. Resulting horizontal and vertical GMRS and FIRS then both achieve the same target performance goals. As with the horizontal site-specific hazard, regarding the range in the reference site hazard, accuracy in the vertical hazard requires a wide integration range over the site-specific horizontal hazard. As a result, to achieve an AEF of  $10^{-6}$  for the vertical site-specific hazard requires the reference site hazard to an AEF of  $10^{-8}$ .

#### 3.4.1 Optimum Number of Realizations

Ideally the objective of the randomization process is to develop statistically stable estimates of median values and standard deviations with as few analyses as possible. Bazzurro and Cornell (2004) suggest that as few as 10 realizations are sufficient for application of Approach 3. As Table 3 suggests, simple statistics indicates stability is a slowly varying function of sample size, particularly for standard deviations. For a tolerance of the statistical sample being within 20% of the population standard deviation at the 90% confidence level, the number of samples is 30 and naturally less for median estimates. Because sigma ( $\ln$ ) is less than 1, typically around 0.1 to 0.4, and it enters as  $\sigma_{\ln}^2$  (e.g. Equation 7), its impacts are generally not large. As Table 3 indicates, improving the accuracy in the aleatory variability to 10% requires a four-fold increase in sample size to 130 realizations at the 90% confidence level. These trends are reflected in Figure 8, which shows the range in median and sigma estimates computed for various sample sizes with five different random seeds. In general, neither median nor sigma estimates are truly stable for fewer than about 200 realizations. Such observations led to 300 realizations to achieve less than a 10% error in sigma estimates in NUREG/CR-6728. In that research exercise, high accuracy was desired as comparisons were made between Approaches 2, 3, and 4. Achievement of similar accuracy in development of hazard consistent UHRS is simply not warranted in view of the impact on computed transfer functions. As both the simple statistics and Figure 8 show, doubling the number of realizations from 30 to 60 does not generally result in a significant improvement in accuracy. Increasing the number of samples beyond 100, as Figure 8 illustrates, is required to achieve highly stable results.

However, it is really the desired accuracy in the computed hazard which should inform the number of samples required. Based on Equation 7 (Section 3.3), for a given percent accuracy in amplitude, the required accuracy in the standard deviation depends on the slope of the reference hazard curve as well as the degree of nonlinearity through the slope of the amplification factors  $C$ . For the Lee Nuclear Station Unit 1 profile, since it is linear,  $C$  becomes zero and from Figure 13, the slope of the reference (hard rock) hazard curve is a

bit less than 2, and the  $\sigma_{in}$  is about 0.1. In this case, the exponential term containing  $\sigma_{in}$  in Equation 7 has a value of about 1.01. A 100% increase in  $\sigma_{in}$  results in a value of about 1.04, or a 3% change. At the 90% confidence level, fewer than 5 realizations are required (30 were run for the Lee Nuclear Station Unit 1 analyses), increasing to fewer than 13 at the 99% confidence level and of course fewer still for estimates of the mean. Conversely, for a  $\sigma_{in}$  near 0.5, a steep hazard curve slope near 4, and over a highly nonlinear loading level (e.g. over 1g at 10 Hz in Figure 6) with  $C$  near 0.5, the exponential term is about 2.7. In this case a 10% increase in  $\sigma_{in}$  results in an exponential value of about 3.4, or about a 20% increase in amplitude, which is significant. For cases such as these, to achieve a 10% accuracy in amplitude requires better than a 5% accuracy in  $\sigma_{in}$ . From Table 3 the number of samples increases from fewer than 5 to 550 at the 90% confidence level to over 1,000 at the 99% confidence level. Clearly, for application of fully probabilistic approaches to developing site-specific hazard, the number of realizations should be case specific and determined with preliminary analyses. For the deterministic approach, since the mean is given by the median times an exponential of  $\sigma_{in}^2$  divided by 2, to achieve a 10% accuracy in the mean requires only about a 30% accuracy in  $\sigma_{in}$ , or about 15 realizations at the 90% confidence limit, 35 samples at the 99% confidence limit.

### **3.4.2 Example Illustrations**

A straightforward way to illustrate the fully probabilistic Approach 3 is through comparisons with the Approximate method (Equation 7) as well as a fully deterministic method using a median amplification. As previously discussed, the approximation renders the full integration quite transparent and it is easy to illustrate the impacts of median amplification, slope of the reference site hazard curve, and amplification variability ( $\sigma_{in}$ ) with simple cases.

#### **3.4.2.1 Illustration Using a Horizontal or Vertical Mock Reference Hazard Curve**

To clearly demonstrate Approach 3, the results of the simplest case of a linear (i.e.  $C = 0$  in Equation 7) reference hazard curve and a linear median amplification or V/H ratio of 2.0 is considered in Figure 9. The aleatory variability of the amplification is taken as 0.2 ( $\sigma_{in}$ ) and the slope of the reference hazard curve is 3 (log-log) initially then increased to an extreme value of 6. Figure 9 compares three derived hazard curves obtained using: Approach 3 full integration (Equation 5), Approach 3 Approximate (Equation 7), and simply median amplification or V/H ratio (2.0) times the reference hazard. For horizontal components, this latter (deterministic) curve effectively reflects Approach 2, which would use the mean amplification. However for this example, the mean is only 2% larger than the median. In general, it is clear that for a slope near 3, there is little difference between the deterministic and fully probabilistic results. The Approach 3, full integration method, results in the largest motions for a given AEF with the results using the approximate fully probabilistic method very slightly lower. For the steeper slope, it is easy to see from Equation 7 the expected impacts of Approach 3. The exponential term in Equation 7 becomes larger for the steeper (by a factor of 2) slope, resulting in the difference between the median deterministic amplification and fully probabilistic Approach 3 becoming significant, approaching 15 to 20%.

Increasing the amplification variability to 0.4 ( $\sigma_{in}$ ) (Figure 10), now shows a substantial difference between deterministic and fully probabilistic results: a difference near 25% for a slope of 3 and nearly 70% for an extreme case with a slope of 6. Use of the mean amplification would only increase the corresponding soil hazard curve by about 8%, leaving it a full 15% below the fully probabilistic Approach 3, illustrating the recommendation in

NUREG/CR-6728 for enveloping high- and low-frequency mean amplification factors as an empirical means of conservatively maintaining the desired hazard level.

This simple example also serves to illustrate the inherent stability of the Approach 3 full integration method. In both Figures 9 and 10, near the discontinuity in slope of the reference site hazard curve (going from a slope of 3 to a slope of 6), the derivative of the reference hazard curve is undefined (very large), causing the observed bulge in the hazard curve computed using the approximate Approach 3 method. The full integration method simply integrates through the singularity, resulting in a gradual change in slope of the resulting soil hazard curve. Because real hazard curves can not have such discontinuities, this extreme case illustrates the appropriateness of the numerical differentiation (e.g. density of points in the hazard reference site hazard curve) as well as the numerical integration scheme employed.

Also apparent in Figures 9 and 10 is the breakdown of the Approach 3 full integration method near the limits of the reference site (input) hazard curve. At low AEF ( $10^{-10}$ ), the reference hazard curve extends to  $10^{-11}$  AEF so the Approach 3 full integration hazard is correct to an AEF of  $10^{-10}$ , as is evident in Figures 9 and 10. However, at high exceedance frequency, the reference site hazard curve extends to an AEF of  $10^{-1}$ . Near this AEF, the Approach 3 full integration hazard shows a decreasing slope and convergence to the reference site hazard. The full integration method simply reflects decreasing contributions to the integral (sum, Equation 5) as the limit of the reference site hazard curve is approached.

#### **3.4.2.2 Illustration Using a Horizontal or Vertical Realistic Reference Hazard Curve**

While the previous simplified example case gave a clear illustration of using the full integration and approximate Approach 3 through examining the differences between deterministic and fully probabilistic approaches to developing UHRS, further insights can be provided by a more realistic case. For this example, a real WNA reference site hazard curve for peak acceleration was used and serves to illustrate the impact of increasing slope of the reference site hazard curve on developing fully probabilistic site-specific motions. As can be seen in Figure 11, the reference site hazard curve has a slope which increases significantly with decreasing AEF. As with the previous example, median amplification or V/H ratio is set at 2.0 and is taken as linear (again  $C = 0$  in Equation 7). Figure 11 illustrates the effect of increasing slope of the reference site hazard curve as the AEF decreases for a range in amplification aleatory variability ( $\sigma_{in} = 0.1$  to 0.4). From Figure 11 it is easy to appreciate the impacts of the exponential term in Equation 7, the increase in motion for a fully probabilistic analysis compared to a deterministic approach, as both the slope and  $\sigma_{in}$  increase. For a typical  $\sigma_{in}$  in the range of 0.3, accommodating aleatory variability in velocities, depth to basement, and modulus reduction and hysteretic damping curves across a site, the difference between the median deterministic soil hazard curve and the fully probabilistic hazard curve is about 25% near the AEF of  $10^{-4}$ . Recall that this example, as well as the last one, assumes linear response in order to provide a more transparent illustration. Consequently the exponential term in Equation 7 is a minimum, resulting in a minimum difference between deterministic and fully probabilistic methods.

Figure 12 illustrates the comparison between deterministic and fully probabilistic analysis results including the approximate Approach 3 method. A typical  $\sigma_{in}$  value of 0.3 is considered and the results illustrated in Figure 12 shows good agreement between the full integration and approximate methods to an AEF of about  $2 \times 10^{-5}$ . Below this exceedance

frequency the approximate method breaks down in this example as the exponential term is becoming too large (Bazzurro and Cornell, 2004).

This example also provides a check on the implementation of the full integration method in terms of differencing the reference site hazard curve (density of points) as well as the numerical integration procedure (Simpson's Rule). The full integration method agrees quite well with the approximate result over AEF where it is expected to do so. At high probability, the reference site hazard curve slope is quite small so the deterministic and fully probabilistic approaches should agree (see Equation 7).

#### **3.4.2.3 Illustration for The Lee Nuclear Station Unit 1 Horizontal UHRS**

The Lee Nuclear Station Unit 1 has approximately 20 ft of concrete ( $V_s = 7,500$  ft/sec) overlying CENA generic rock ( $V_s \approx 9,300$  ft/sec). In developing the amplification factors for Unit 1, the thickness in the concrete was varied  $20 \text{ ft} \pm 3 \text{ ft}$  and velocities were randomly varied using a typical concrete coefficient of variability (COV) of 0.1. Due to the profile stiffness, a linear analysis was used in developing the amplification factors (Figure 2). Also, due to the linear analysis, the typical dense grid of expected reference site peak accelerations (Table 2) was not needed. Instead, to examine any potential impacts of spectral shape on 5% damped response spectra and thereby amplification factors due to crustal damping at large distances ( $> 100$  km), a coarse distance grid spanning 1 km to 400 km was used (Figure 2). While the expected amplification due to the concrete fill is well above 50 Hz (resonance near 90 Hz), some amplification may propagate to frequencies of potential structural concern, below 50 Hz. This may be due not only to the variability, randomness in dynamic material properties, but also the smoothing aspect of 5% damped response spectra. Recall that at high-frequency, response spectra, being a constant damping smoothing operator, reflect transfer functions or resonances that are extremely wide. Depletion of reference site energy at high-frequency due to crustal damping at large distance ( $> 100$  km) may cause the amplification factor resonance to shift to lower frequency.

Figure 2 reveals this is not an issue of concern as there is only a very minor difference between the amplification factors computed at 1 and 400 km. As a result, any of the suite of amplification factors may be used.

Also, for the Lee Nuclear Station Unit 1, because of the linear response, the amplification factors are, by definition, independent of reference site spectral shape due to magnitude as well as single- or double-corner source spectral shapes. For this case, Approaches 1 and 2 are identical.

As a result, based on our previous examples, Approach 3 (without the correction factors, Section 3) as applied to the Lee Nuclear Station Unit 1 becomes trivial and reflects an excellent illustration case. An additional benefit in transparency of Approach 3 applied to the Lee Nuclear Station Unit 1 is the unusually small aleatory variability due to the typical uniformity of concrete properties (COV = 0.1). The resulting  $\sigma_{ln}$  is about 0.1 giving a mean to median ratio of only 1.005. This result indicates that the mean amplification over the median amplification (Figure 11) is only about 0.5%, virtually the same. As a consequence a fully probabilistic method, Approach 3 analysis, due to linear site response ( $C = 0$  in Equation 7) and a very small aleatory variability ( $\sigma_{ln} \approx 0.1$ , see Figure 11) should give results very similar to a deterministic method (Approaches 1 and 2 in this case), provided the hard rock hazard curve does not have a steep slope.

To illustrate the deterministic and probabilistic approaches applied to the Lee Nuclear Station Unit 1, Figure 13 shows the hard rock (reference site) mean hazard curve computed for peak acceleration. Over the AEFs of interest in the integration,  $10^{-3}$  to  $10^{-6}$ , to define the site UHRS at AEFs of  $10^{-4}$  and  $10^{-5}$ , the slope of the hazard curve is about 2, or slightly less. Comparing the "deterministic UHRS" computed by multiplying the median amplification factor at 50 km (Figure 2) times the hard rock AEF  $10^{-4}$  mean UHRS with the fully probabilistic Approach 3 method, Figure 14 shows the expected equivalence. The two approaches yield very nearly identical results, as expected for a linear analysis, small  $\sigma_{ln}$ , and gently sloping reference site hazard curve. Figure 15 shows similar results computed for an AEF of  $10^{-5}$ .

In summary, the Lee Nuclear Station Unit 1 reflects a clear and transparent application of the fully probabilistic Approach 3 method to achieve hazard consistent horizontal and vertical UHRS. The Unit 1 site properties are such that the fully probabilistic method reduced to a classical deterministic method is well illustrated by the approximate Approach 3 method in the previous test cases.

#### **4.0 APPLICATION TO VERTICAL HAZARD**

Typically the vertical UHRS is developed by a deterministic application of V/H ratios applied to the horizontal UHRS. Since V/H ratios vary with both magnitude and distance for sites with nonlinear response and with distance for linear sites (e.g. hard rock) (Silva, 1997; NUREG/CR-6728), it is essential to capture these dependencies, identified through model deaggregations, in developing the vertical UHRS. For the deterministic approach, paralleling Approach 2 for the horizontal motions (Section 3.0), conservative estimates of appropriate V/H ratios must be used to ensure achievement of the same hazard levels and target performance goals as the horizontal UHRS. Additionally, V/H ratios reflect epistemic variability as is evidenced by WNA empirical soft rock and deep firm soil V/H ratios (Abrahamson and Shedlock, 1997), further pointing out the necessity of conservatism in a deterministic approach to developing vertical UHRS. As previously discussed in the context of Approach 2 for the horizontal UHRS, incorporation of epistemic variability in a deterministic framework is not unambiguous as one can not simply average over suites of motions or transfer functions which reflect epistemic variability. This process will not generally achieve desired hazard levels and reliance on conservatism in V/H ratios remains the most reliable option. These considerations, along with a desire for easy implementation as a function of expected horizontal peak acceleration, led to the purposeful incorporation of conservatism in development of the CENA hard rock V/H ratios (NUREG/CR-6728).

To accurately achieve desired hazard levels as well as performance goals, a fully probabilistic approach is used, directly paralleling that for the horizontal hazard. Implementation of the full integration Approach 3 (Section 3.2) for vertical hazard simply substitutes V/H ratios for horizontal amplification factors. In this case, the distribution of V/H ratios are integrated with the horizontal site-specific hazard curves (presumably developed using Approach 3). As with the horizontal case, Approach 3 then admits the proper and unambiguous incorporation of both aleatory and epistemic variabilities in V/H ratios, achieving desired hazard levels. Again, in parallel with development of the horizontal hazard, model deaggregations are used but, as previously stated, in addition to magnitude, source distance is required as V/H ratios depend on distance as well as magnitude for soil or soft rock site conditions.

#### 4.1 Hazard Deaggregation For The William States Lee III Nuclear Station

Figure 16 shows the source contributions in magnitude and distance for the Lee Nuclear Station. In general there are three controlling sources: background sources with  $M$  near 5 and within about 20 to 40 km, the Charleston, South Carolina source zone with  $M$  near 7 and around 250 km distance, and the New Madrid source zone over 400 km distance and with  $M$  around 8. For high-frequencies, 5 Hz to 10 Hz and above, as AEF decreases from  $10^{-4}$  to  $10^{-5}$  and  $10^{-6}$ , the background source becomes much more dominant and concentrates within about 20 km of the site at an AEF of  $10^{-6}$ . At low frequency, 1 Hz to 2.5 Hz, distance sources dominate at AEF of  $10^{-4}$  to  $10^{-5}$ . At  $10^{-6}$  AEF and at 1 Hz to 2.5 Hz, the background source within 20 to 40 km becomes more significant, controlling the peak in the deaggregation, although distant source have significant contributions.

It is these general trends that are intended to be captured in applying the magnitude and distance dependent V/H ratios to the horizontal hazard.

#### 4.2 Development of V/H Ratios

In the following sections the development of site-specific ratios and the motivation for inclusion of empirical V/H ratios is presented.

##### 4.2.1 Site-Specific V/H Ratios

To develop site-specific vertical motions, incident inclined P-SV waves are modeled from the source to the site using the plane-wave propagators of Silva et al. (1976) assuming a shear-wave point-source spectrum (Boore; 1983, 2003). The point-source model is used to accommodate the effects of source distance and source depth on V/H ratios. For consistency, both the horizontal and vertical motions are modeled using the same source and path parameters (Table 2). The horizontal motions are modeled as vertically propagating shear-waves. For the vertical motions, the angles of incidence are computed by two-point ray tracing through the crust and site-specific profile. To model site response, the near-surface  $V_P$  and  $V_S$  profiles are placed on top of the crustal structure, the incident P-SV wavefield is propagated to the surface assuming a linear analysis, and the vertical motions are computed. For the Lee Nuclear Station Unit 1 with 20 ft of concrete over hard rock (Table 2), the base-case shear- and compressional-wave velocities are 7,500 ft/sec and 14,000 ft/sec respectively.

For typical crustal structures without strong near-surface  $V_P$  gradients and at close distances, the predominant motion on the vertical component is principally due to the SV wavefield. In a soil column (particularly deep profiles), however, because there is usually a large  $V_P$  gradient (larger for P-waves than for S-waves as Poisson ratios generally decrease with increasing depth), the vertical component is usually controlled by the compressional wavefield at high frequency (Silva, 1997; Amirbekian and Bolt, 1998; Beresnev et al., 2002).

In the implementation of the equivalent-linear approach to estimate V/H response spectral ratios, the horizontal component analyses are performed for vertically propagating shear-waves. To compute the vertical motions, a linear analysis is performed for incident inclined P-SV waves using low-strain  $V_P$  and  $V_S$  derived from the base-case profiles. The P-wave damping is assumed to be equal to the low strain S-wave damping (Johnson and Silva, 1981). The horizontal component and vertical component analyses are assumed to be independent.

The approximations of linear analysis for the vertical component and uncoupled vertical and horizontal components have been validated in two ways. Fully nonlinear modeling using a 3-D soil model shows that the assumption of largely independent horizontal and vertical

motions for loading levels up to about 0.5g (soil surface, horizontal component) for moderately stiff profiles is appropriate (EPRI, 1993). Additionally, validation exercises with recorded motions have been conducted at over 50 sites that recorded the 1989 **M** 6.9 Loma Prieta and 1992 **M** 6.7 Northridge earthquakes (EPRI, 1993). These validations show the overall bias and variability is acceptably low for engineering applications but is higher than that for horizontal motions. The vertical model does not perform as well as the model for horizontal motions (EPRI, 1993; Silva, 1997). An indirect validation was also performed by comparing V/H ratios from WNA empirical attenuation relations with model predictions over a wide range in loading conditions (Silva, 1997). The results show a favorable comparison with the model exceeding the empirical V/H ratios at high frequency, particularly at high loading levels. In the V/H comparisons with empirical relations, the model also shows a small under prediction at low frequency ( $\leq 1$  Hz) and at large distance ( $\geq 20$  km).

For the vertical analyses, a hard rock kappa value of 0.003 sec, half that of the horizontal, is used. This factor of 50% is based on observations of kappa at strong motion sites (Anderson and Hough, 1984), validation exercises (EPRI, 1993), as well as the observation that the peak in the vertical spectral acceleration (5% damped) for WNA rock and soil sites is generally near 10 to 12 Hz compared to the horizontal motion peak that occurs at about 5 Hz, conditional on **M** 6.5 at a distance of about 10 to 30 km (Abrahamson and Silva 1997; Campbell 1997; Campbell and Bozorgnia 2003). This difference of about 2 in peak frequency is directly attributable to differences in kappa of about 2. Similar trends are seen in CENA hard rock spectra with the vertical component peaking at higher frequencies than the horizontal component.

The site-specific V/H ratios are shown in Figure 17 and reflect median estimates computed with the stochastic model for **M** 5.1. As previously discussed, due to the stiffness of the Unit 1 profile, linear analyses were performed for the horizontal component resulting in magnitude independent amplification factors and V/H ratios. For **M** 5.1, the distances range from 80 to 0 km (Table 2) with expected horizontal hard rock peak accelerations ranging from 0.01 to 0.50g. As Figure 17 shows, the V/H ratios for the shallow concrete profile of Unit 1 are nearly constant with frequency and increase rapidly as distance decreases, within about a 15 km source distance. For distances beyond 10 to 15 km, the V/H ratio is about 0.5 and increases rapidly to about 0.9 within about 5 km. The peak near 60 Hz is likely due to the peak in the vertical spectra. The multiple peaks beginning near 1 Hz reflect deep crustal resonances (structure below a depth of 1 km, Table 2) and would be smoothed if the crustal model were randomized and discrete layers replaced with steep velocity gradients to reflect lateral variability and a more realistic crustal structure. The distance ranges more than adequately accommodate the hazard deaggregation.

As previously discussed, the model predictions of V/H ratios at low-frequency may be slightly unconservative and at high frequency they may be conservative. While it is important to include site-specific effects on the vertical hazard, potential model deficiencies may be compensated with inclusion of empirical V/H ratios computed from WNA generic rock attenuation relations (Section 4.2.2). Additionally, empirical V/H ratios of Fourier amplitude spectra based on CENA recordings at hard rock sites for small magnitudes and at very large distances have median values near about 0.8 and vary slowly with frequency (Gupta and McLaughlin, 1987; Atkinson, 1993). To accommodate potential model deficiencies as well as the large uncertainty in hard and firm rock V/H ratios for CENA, a minimum value of 0.7 is adopted, the average of the empirical CENA and site-specific V/H ratios at large distance ( $> 20$  km).

#### 4.2.2 Empirical V/H Ratios

Empirical western North America V/H ratios for soft rock are included in the development of vertical motions in addition to site-specific point-source simulations. The use of WNA empirical V/H ratios implicitly assumes similarity in shear- and compression-wave profiles and nonlinear dynamic material properties between site condition in WNA and the Lee Nuclear Station Unit 1 column (Silva et al., 1999). Whereas this may not be the case for the average WNA rock site profile (Silva, 1997), the range in site conditions sampled by the WNA empirical generic rock relations likely accommodates site-specific conditions. The relative weights listed in Table 4 reflect the assumed appropriateness of WNA soft rock empirical V/H ratios for Unit 1. Additionally, because the model for vertical motions is not as thoroughly validated as the model for horizontal motions (EPRI, 1993), inclusion of empirical models is warranted. The additional epistemic variability introduced by inclusion of both analytical and empirical models also appropriately reflects the difficulty and lack of consensus regarding the modeling of site-specific vertical motions (EPRI, 1993). In the implementation of Approach 3 to develop vertical hazard curves, the epistemic variability is properly accommodated in the vertical mean UHRS, reflecting a weighted average over multiple vertical hazard curves computed for Unit 1 using multiple models. The vertical FIRS (and UHRS) then maintain the desired risk and hazard levels, consistent with the horizontal UHRS.

For the empirical V/H ratios, both Abrahamson and Silva (1997) and Campbell and Bozorgnia (2003): Bozorgnia, and Campbell (2004) soft rock WNA relations are used with equal weights (Table 4). As an example, Figure 18 shows the Campbell and Bozorgnia V/H ratios computed for  $M$  5.1 and  $M$  8.0. Distance bins differ between the empirical and analytical V/H ratios because the empirical ratios use a generic suite of distances used on several projects while the analytical V/H ratios are region specific. For distances beyond 57 km, the empirical V/H ratios are nearly constant with increasing distance. Additionally, for the smaller  $M$  ( $M < 5.5$ ), there are few strong motion data available at larger distances (Campbell and Bozorgnia, 2003). Because the ratios vary slowly with distance, the differences in distances are not significant. The empirical WNA soft rock ratios show more distance (loading level) dependence than the site-specific analytical ratios (Figure 17), perhaps due to nonlinearity in the horizontal soft rock motion (Silva, 1997). These trends, with the  $M$  independence of V/H ratios, are expected for firm rock conditions. That is, as the profile becomes stiffer, nonlinearity decreases, and for distances within about 10 to 15 km, distance becomes the dominant controlling factor in V/H ratios (Silva, 1997).

The empirical soft rock V/H ratios show a clear dependency on magnitude, although it is not particularly strong as the comparison is over magnitude 5.1 and 8.0. The distance dependency for the empirical V/H ratios shown in Figure 18 clearly illustrates epistemic variability having significantly different trends with distance between those of Abrahamson and Silva (1997) and Campbell and Bozorgnia (2003). As an example, at 20 Hz and for  $M$  5.1, Abramson and Silva (1997) show little distance dependency with a value near 0.7 while Campbell and Bozorgnia (2003) show a range varying from about 0.6 to about 1.0, about a 70% change, over the distance range of 57 km to 1 km. The converse is apparent for  $M$  8.0. Such differences between relations generally considered reliable illustrate the significant epistemic variability inherent in developing vertical hazard and the necessity for its statistically proper inclusion through the use of multiple models, within the context of Approach 3 (Section 3.0).

It is important to note the site-specific and generic V/H ratios peak at very different frequencies, about 60 Hz and about 10 to 20 Hz, respectively, with the site-specific having generally higher V/H ratios, particularly at close distances. Use of an empirical V/H ratio



alone may underestimate the vertical hazard at high frequency, provided the model predictions are reasonably accurate.

For the empirical V/H ratios, to fully accommodate the hazard deaggregation (Section 4.1, Figure 16), V/H ratios for magnitude 7.0 were also computed and used (Table 4) in developing the vertical hazard (Section 4.3).

#### **4.2.3 Aleatory Variability In V/H Ratios**

In addition to the epistemic variability accommodated through the use of multiple models for V/H ratios, aleatory variability due to randomness of dynamic material properties varying vertically and laterally across the site should be accommodated as well. However, in developing the vertical hazard, since site-specific aleatory variability has been incorporated in developing the horizontal site-specific hazard curves, it is advisable to constrain the sigma of the site-specific V/H ratios to values less than about 0.15 to 0.20 ( $\sigma_m$ ). This range is to accommodate the observation of slightly larger variability about median attenuation relations in the vertical component compared to the horizontal component (Abrahamson and Silva, 1997). An example of aleatory variability in site-specific V/H ratios computed for the Lee Nuclear Station Unit 1 is shown in Figure 19 (80 km case, Figure 17). For the Unit 1 site conditions and hard rock in general, the aleatory variability is quite small, less than about 0.1 ( $\sigma_m$ ) due to the COV of 0.1 for shear-wave velocity within the concrete. However for less uniform materials, the standard deviation can be significantly larger; as a result, limiting its value avoids potential double counting site-specific aleatory variability in developing vertical hazard. It should be noted that for the computation of site-specific V/H ratios, the denominator (horizontal component) should be taken as the median (i.e. not varied) and multiple realizations of the vertical component taken to form the basis for the aleatory variability in the V/H ratios. This approach is intended to properly isolate the variability in the V/H ratios to that of the verticals, recognizing the variability in the horizontal component has already been accommodated in the randomization of shear-wave dynamic material properties.

The occasion to limit the V/H ratio variability may arise due to the randomization process incorporated in the model for the vertical motions. For simplicity, the randomization of the compressional-wave velocities fixes the Poisson ratios in the profile at the values of the base-case shear- and compressional-wave velocities. The profile randomization scheme (Section 2.2.1), based on shear-wave velocities and layer thickness, produces realizations of shear-wave velocities with corresponding compressional-wave velocities using the original Poisson ratios. This process results in a suite of random shear- and compressional-wave profiles, all with the same Poisson ratios (verses depth). It may very well be the case this simplifying assumption results in too large a range in compressional-wave velocities, perhaps due to a coupling between shear-wave velocity and Poisson ratio. Obviously, because horizontal components and consequently shear-waves are of major concern and because there are many more measured shear-wave velocity profiles than both shear- and compressional-wave velocity profiles, the profile randomization scheme has concentrated on shear-waves. Additionally, a more statistically correct compressional-wave randomization scheme would have little impact as a 20% to 30% change in the aleatory variability, if small, has a very minor impact (3% to 4%) on the vertical hazard for typical ranges in the slope ( $\kappa$ ) of the horizontal hazard curve (2 to 6) and slope of the V/H ratios with loading level (distance), as illustrated in Equation 7.

Returning to the empirical V/H ratios, Figure 18, as only median estimates are available through horizontal and vertical attenuation relations (Abrahamson and Silva, 1997;

Campbell and Bozorgnia, 1994, 2003), in application of Approach 3 which requires aleatory variability (e.g. Equation 7) in the V/H ratios, a value of 0.15 ( $\sigma_{in}$ ) is used.

### 4.3 Implementation of V/H Ratios In Developing Vertical Hazard

In assigning the V/H ratios in the Approach 3 analysis, the source  $M$  and  $D$  change significantly with structural frequency as exceedance frequency changes (Section 4.1, Figure 16). To accommodate the deaggregation in (contributing sources) integrating the horizontal hazard with the distributions of V/H ratios, the  $M$  and  $D$  selection follows that listed in Table 4. The magnitudes selected are intended to capture the dominant sources:  $M$  5.1 for close-in sources and  $M$  7.0 and  $M$  8.0 for the Charleston, South Carolina and New Madrid, Missouri sources, respectively, both at distances well beyond 100 km. The distances used for the V/H ratios (Table 4) reflect the distance sensitivity, or lack of sensitivity beyond about 10 to 15 km for the site-specific ratios and beyond about 50 km for the empirical ratios, considering the contributing source distances. The weights listed in Table 4 are intended to approximate the relative contributions of the three sources across structural frequency and exceedance probability. Because the V/H ratios vary slowly with distance, only a smooth approximation to the hazard deaggregation is necessary. To adequately capture the change in  $M$  and  $D$  with AEF, only a few distance bins are required: 5 and 57 km for the empirical V/H ratios and 0, 7, and 28 km for the analytical V/H ratios (Table 4).

To illustrate the vertical hazard computed using Approach 3 with the empirical and site-specific V/H ratios, Figure 20 shows horizontal and vertical UHRS computed for the Lee Nuclear Station Unit 1 profile for AEF  $10^{-4}$ ,  $10^{-5}$ , and  $10^{-6}$ . The magnitude and distance deaggregation (Figure 16, Section 4.1) is seen to be captured in the apparent V/H ratios (vertical UHRS divided by the horizontal UHRS). As the AEF decreases and both the high- and low-frequency source contributions move closer to the site (Table 4, Figure 16), higher weight is placed on the closer empirical and site-specific V/H ratios resulting in larger apparent V/H ratios. The fully probabilistic approach then results in hazard consistent vertical UHRS that properly accommodate site-specific aleatory and epistemic variability as well as the effect of magnitude and distance on vertical motions. This is especially the case at high-frequency and low AEF at  $10^{-6}$ .

#### 4.3.1 UHRS Interpolation and Extrapolation

Because the reference (hard rock) hazard is computed at only seven frequencies, namely 0.5, 1.0, 2.5, 5.0, 10.0, 25.0, and 100.0 Hz (taken as peak acceleration), the site-specific hazard has been both extrapolated to 0.1 Hz and at high-frequency, the reference hazard curves were interpolated at 34 and 50 Hz, as these are the critical frequencies to define the Unit 1 UHRS shapes beyond 25 Hz. The interpolation is performed by using the deterministic shapes (NUREG/CR-6728) for the appropriate  $M$  to interpolate the hard rock UHRS at AEF of  $10^{-4}$ ,  $10^{-5}$ , and  $10^{-6}$  yr<sup>-1</sup>, resulting in three points on 34 and 50 Hz hazard curves. The adjacent hazard curves at 25 and 100 Hz are then used as shapes to extrapolate to lower and higher exceedance probabilities, resulting in approximate hard rock hazard curves. Approach 3 is then applied to develop site-specific horizontal and vertical UHRS at the same exceedance frequency as the 25 Hz and 100 Hz hard rock hazard curves. Approach 3 (full integration method) is then applied to develop site-specific horizontal and vertical UHRS at the same exceedance probability as the 25 and 100 Hz hard rock hazard. For the vertical component, because the site-specific V/H ratios peak at very high-frequency (beyond 50 Hz), it is important to maintain the appropriate hazard levels between 25 and 50 Hz.

Below 0.5 Hz, because the aleatory variability in attenuation relations increases with period (Abrahamson and Shedlock, 1997; EPRI, 2004), use of a median spectral shape (NUREG/CR-6728) to extrapolate at low-frequency may be inappropriate and result in potentially unconservative hazard or higher probability than desired. To address this uncertainty, a conservative approach is adopted by extrapolating the 0.5 Hz  $10^{-4}$ ,  $10^{-5}$ , and  $10^{-6}$  hard rock UHRS, assuming a constant slope in spectral velocity (+1 slope in pseudo-absolute spectral acceleration) (BSSC, 2004). The extrapolation is extended at low-frequency to the earthquake source corner frequency, where the slope is increased to a constant spectral displacement. Since the source corner frequency, or transition from approximately constant spectral velocity to spectral displacement, depends on magnitude, an average representative magnitude of **M** 7.2 is assumed to apply for frequencies below 0.5 Hz, based on the low-frequency deaggregation (Figure 16). Application of the empirical relation

$$\text{Log } T = -1.25 + 0.3 \text{ M} \quad (8)$$

(BSSC, 2004) results in a corner period (**T**) of approximately 8 sec (0.125 Hz). To accommodate this expected change in slope, the extrapolations are performed at 0.125 and 0.1 Hz, assuming constant spectral velocity from 0.5 to 0.125 Hz and constant spectral displacement for frequencies below 0.125 Hz.

## 5.0 CONCLUSIONS

For the Lee Nuclear Station Unit 1, a fully probabilistic methodology (Approach 3) was used to develop the site-specific UHRS (NUREG/CR-6728 and 6769). As part of this approach, site-specific amplification factors as well as V/H ratios were developed using RVT (NUREG/CR-6728), rather than time domain analyses (e.g. SHAKE).

As part of the acceptance review of the William States Lee III Nuclear Station Combined License Application, the NRC indicated that FSAR Section 2.5.2 did not provide a sufficient level of detail describing the Approach 3 methodology and how the methodology was used with RVT to develop the final site ground motions. To address these comments, this document presents a full and complete development of both RVT, in applications to site response and V/H ratios, as well as both deterministic (Approaches 1 and 2) and probabilistic (Approaches 3 and 4) methods to developing site-specific UHRS.

Regarding site response, the two areas where RVT is used directly in estimating response spectra and peak shear strains for equivalent-linear analyses have been presented and discussed. Other related considerations in site response such as choice of control motion, effects of control motion spectral shape, and incorporation of aleatory variabilities in dynamic material properties have been presented and discussed in terms of potential impacts to the development of site-specific UHRS. Additionally, general guidelines for implementing RVT in terms of site response have been presented and discussed.

All four methodologies for developing site-specific ground motions (Approach 1 to 4) have been presented and discussed in order of increasing accuracy and complexity. The fully probabilistic approach used in computing the Lee Nuclear Station Unit 1 UHRS (Approach 3) was developed through the derivation of basic equations, illustrating the various simplifications as well as assumptions. Also presented and discussed are implementation limitations of Approach 3 as well as the other approaches, and how these limitations are addressed to preserve accuracy, or conservatism in the case of deterministic approaches, in computing site-specific hazard curves. Sensitivities of the fully probabilistic approach to

various parameters have also been explored to illustrate the essential elements in the methodology, which enables the approach to achieve hazard consistency. Also presented is a discussion of the optimum number of site response realizations, in terms of confidence levels, to achieve a given accuracy in ground motion at a given hazard level for implementation of the fully probabilistic approach.

Finally, Lee Nuclear Station Unit 1 specific parameter values and results have been presented for the horizontal and vertical UHRS.

## 6.0 REFERENCES

- Abrahamson, N.A. and W.J. Silva (1997). "Empirical response spectral attenuation relations for shallow crustal earthquakes." *Seismological Research Letters*, 68(1), 94-127.
- Abrahamson, N.A. and K.M. Shedlock (1997). "Overview." *Seismological Research Letters*, 68(1), 9-23.
- Amirbekian, R.V. and Bolt, B.A. (1998). "Spectral comparison of vertical and horizontal seismic strong ground motions in alluvial basins." *Earthquake Spectra*, 14(4), 573-595.
- Anderson and Hough, 1984 Anderson, J. G. and S. Hough (1984). A Model for the shape of the Fourier amplitude spectrum of acceleration at high frequencies: *Bulletin Seismological Society of America*, 74, 1969-1994
- Atkinson, G.M. and W.J. Silva (1997). "An empirical study of earthquake source spectra for California earthquakes." *Bulletin of Seismological Society of America*, 87(1), 97-113.
- Atkinson, G.M. (1993). "Notes on ground motion parameters for eastern North America: duration and H/V ratio." *Bulletin of Seismological Society of America*, 83(2), 587-596.
- Bazzurro, Paolo and C.A. Cornell (2004). "Nonlinear soil-site effects in probabilistic seismic-hazard analysis." *Bulletin of Seismological Society of America*, 94(6), 2110-2123.
- Beresnev, I.A, Nightengale, A.M. Silva, W.J. (2002). "Properties of vertical ground motions." *Bulletin of the Seismological Society of America*, 92(2), 3152-3164.
- Bozorgnia, Y. and Campbell, K. (2004). "The vertical-to-horizontal response spectral ratio and tentative procedures for developing simplified V/H and vertical design spectra" *Journal of Earthquake Engineering*, 8(2), 175-207.
- Boore, D.M. (2003) "Simulation of ground motions using the stochastic method" *Pure and Applied Geophysics*, 160, 635-676.
- Boore, D.M. and Joyner, W.B. (1984). "A note on the use of random vibration theory to predict peak amplitudes of transient signals." *Bulletin of Seismological Society of America*, 74, 2035-2039.
- Boore, D.M. (1983). "Strong-motion seismology." *Reviews of Geophysics*, 21, 1308-1318.
- Building Seismic Safety Council (BSSC) (2004). "National Earthquake Hazards Reduction Program (NEHRP), Recommended Provisions for Seismic Regulations for New Buildings and Other Structures (FEMA 450), Report prepared for the Federal Emergency Management Agency (FEMA).
- Campbell, K W. (1997). "Empirical near-source attenuation relationships for horizontal and vertical components of peak ground acceleration, peak ground velocity, and pseudo-absolute acceleration response spectra." *Seismological Society of America*, 68(1), 154-176.

- Campbell, K.W. and Y. Bozorgnia (1994). "Near-source attenuation of peak horizontal acceleration from worldwide accelerograms recorded from 1957 to 1993." in Proceedings, Fifth U.S. National Conference on Earthquake Engineering. Chicago, Illinois. vol. III, p.283-292.
- Campbell, K.W. and Y. Bozorgnia (2003). "Updated Near-Source Ground Motion (Attenuation) Relations for the Horizontal and Vertical Components of Peak Ground Acceleration and Acceleration Response Spectra," Bulletin of the Seismological Society of America, 93 (1):314-331
- Cramer, C. H. (2003) "Site-specific seismic hazard analysis that is completely probabilistic." Bulletin of Seismological Society of America, 93, 1841-1846.
- Duke Energy Carolinas, LLC (2007), William States Lee III Nuclear Station – Project 724, Application for Combined License for William States Lee III Nuclear Station Units 1 and 2.
- Electric Power Research Institute (2004). "CEUS Ground Motion Project Final Report." EPRI, Palo Alto, CA, Dominion Energy, Glen Allen, VA, Entergy Nuclear, Jackson, MS, and Exelon Generation Company, Kennett Square, PA: 2004. 1009684.
- Electric Power Research Institute (1993). "Guidelines for determining design basis ground motions." Palo Alto, California: Electric Power Research Institute, vol. 1-5, EPRI TR-102293.
- Electric Power Research Institute. (1988). "Engineering model of earthquake ground motion for eastern North America." Palo Alto, California: Electric Power Research Institute, EPRI NP-6074.
- Gupta, I.N. and K.L. McLaughlin (1987). "Attenuation of ground motion in the Eastern United States." Bulletin of Seismological Society of America, 77, 366-383.
- Hartzell, S., S. Harmsen, A. Frankel, and S. Larsen (1999). "Calculation of broadband time histories of ground motion: Comparison of methods and validation using strong-ground motion from the 1994 Northridge Earthquake." Bulletin of Seismological Society of America, 89(6), 1484-1504.
- Herrmann, R.B. (1985). "An extension of random vibration theory estimates of strong ground motion to large distance." Bulletin of Seismological Society of America, 75, 1447-1453.
- Idriss, I. M. and H.B. Seed (1968) "Seismic response of horizontal soil layers." Journal of Soil Mechanics and Foundation Engineering, Proceedings of ASCE, Vol. 94, No. 4, pp. 1003-1031.
- Johnson, L.R., and W.J Silva (1981). "The effects of unconsolidated sediments upon the ground motion during local earthquakes." Bulletin of Seismological Society of America, 71, 127-142.

- Lee, R., M. E. Maryak, and J. Kimball (1999). "A methodology to estimate site-specific seismic hazard for critical facilities on soil or soft-rock sites." *Seismological Research Letters*, 70, 230.
- Lee, R., W.J. Silva, and C. A. Cornell (1998). "Alternatives in evaluating soil- and rock-site seismic hazard." *Seismological Research Letters*, 69, 81.
- McGuire, R.K., W.J. Silva and C.J. Costantino (2001). "Technical basis for revision of regulatory guidance on design ground motions: hazard- and risk-consistent ground motions spectra guidelines." Prepared for Division of Engineering Technology, Washington, DC, NUREG/CR-6728.
- McGuire, R.K., W.J. Silva and C.J. Costantino (2002). "Technical Basis for Revision of Regulatory Guidance on Design Ground Motions: Development of Hazard- and Risk-consistent Seismic Spectra for Two Sites." NUREG/CR-6769.
- Pakiser, L.C. and W. D. Mooney (1989). "Geophysical Framework of the Continental United States." *Geological Society of America Memoir* 172.
- Schnabel, P.B., Lysmer, J., and Seed, H.B. (1972). SHAKE: a Computer Program for Earthquake Response Analysis of Horizontally Layered Sites. Earthquake Engineering Research Center (EEEC), University of California at Berkeley, EERC 72-12.
- Schneider, J.F., W.J. Silva, and C.L. Stark (1993). Ground motion model for the 1989 M 6.9 Loma Prieta earthquake including effects of source, path and site. *Earthquake Spectra*, 9(2), 251-287.
- Silva, W. J., S. Li, B. Darragh, and N. Gregor (1999). "Surface geology based strong motion amplification factors for the San Francisco Bay and Los Angeles Areas." A PEARL report to PG&E/CEC/Caltrans, Award No. SA2120-59652.
- Silva, W.J., N. Abrahamson, G. Toro, C. Costantino (1997). "Description and validation of the stochastic ground motion model." Report Submitted to Brookhaven National Laboratory, Associated Universities, Inc. Upton, New York.
- Silva, W.J. and R. Darragh (1995). "Engineering characterization of earthquake strong ground motion recorded at rock sites." Palo Alto, California: Electric Power Research Institute, TR-102261.
- Silva, W.J. (1992). "Factors controlling strong ground motions and their associated uncertainties." *Seismic and Dynamic Analysis and Design Considerations for High Level Nuclear Waste Repositories*, ASCE 132-161.
- Silva, W.J., T. Turcotte and Y. Moriwaki (1986). "Soil response to earthquake ground motions." Palo Alto, Calif.: Electric Power Research Institute, EPRI Research Project RP 2556-07.
- Silva, W.J. (1997). Characteristics of vertical strong ground motions for applications to engineering design, in Proc. FHWA/NCEER Workshop on the National

Representation of Seismic Ground Motion for New and Existing Highway Facilities,  
Technical Report, NCEER-97-0010, National Center for Earthquake Engineering  
Research, Buffalo, New York.

Silva, W.J. (1976). "Body Waves in a Layered Anelastic solid." Bulletin of Seismological  
Society of America, vol. 66(5), 1539-1554.



## 7.0 TABLES AND FIGURES

**TABLES**

Table 1

## Definitions of Locations for Motions in Site-Response Analyses

1. Outcrop: May be specified at the surface or at any depth within a profile.
  - A. Surface Outcrop: All material above the outcrop location is removed. Motion comprised as the sum of upgoing and downgoing waves. For vertically propagating waves (shear or compressional) the free surface effect results in an amplification of exactly 2 over upgoing waves (incident wavefield).
  - B. At-Depth Outcrop: Material above the outcrop location remains in place. Motion comprised of upgoing wavefields only. However the upgoing wavefields at the outcrop location may contain wavefields which propagated above the outcrop location, reflected from impedance contrasts and the free surface, and propagated down past the outcrop location. If there are significant impedance contrasts below the outcrop location, these reflected wavefields contribute to the upgoing wavefields at the outcrop location and may increase or decrease the upgoing wavefield.
2. At Depth In-Column or Total Motions: As with the Outcrop-At-Depth, material above the location of the computed motions remains in place. Motions are comprised of upgoing and downgoing wavefields (total motion) and reflect motions experienced by a buried instrument (e.g. vertical array).
3. Free-Field: Surface or At-Depth motions unaffected to a significant degree ( $\leq 10\%$ ) by the built environment. For recording instruments, this is generally achieved at a foundation dimension away from structures. For in-structure motions, this is achieved at ground level and light structures of two stories or fewer.
4. Site: In this document the term site is used in its classical sense to reflect a single geographical point, rather than the area occupied by a nuclear station.

Table 2 Hard Rock Expected Horizontal Peak Acceleration Levels, Point Source Distances, and Durations					
M 5.1, single-corner					
G(g)	Distance (km)	Depth (km)	T <sub>source</sub> (sec)	T <sub>path</sub> (sec)	T <sub>total</sub> (sec)
1.50	0	2	0.96	0.04	1.00
1.25	0	2	0.96	0.04	1.00
1.00	0	3	0.96	0.05	1.01
0.75	0	4	0.96	0.12	1.08
0.50	0	5	0.96	0.20	1.16
0.40	0	6	0.96	0.25	1.21
0.30	0	8	0.96	0.34	1.30
0.20	7	8	0.96	0.47	1.43
0.10	16	8	0.96	0.84	1.80
0.05	27	8	0.96	1.43	2.39
0.01	80	8	0.96	3.97	4.93

Notes: Additional parameters used in the point-source model are:

$$Q = 670 f^{0.33}$$

$$\Delta\sigma (1c) = 110 \text{ bars}$$

$$\kappa = 0.006 \text{ sec, hard rock}$$

$$\rho = 2.71 \text{ cgs}$$

$$\beta = 3.52 \text{ km/sec}$$

$$R_c = 60 \text{ km, crossover hypocentral distance to } R^{-0.5} \text{ geometrical attenuation}$$

$$T = 1/fc + 0.05 R, \text{ RVT duration, } R = \text{hypocentral distance (km)}$$

CENA Generic Hard Rock Crustal Model			
Thickness (km)	Vs (km/sec)	Vp (km/sec)	$\rho$ (cgs)
1	2.83	4.90	2.52
11	3.52	6.10	2.71
28	3.75	6.50	2.78
[infinite]	4.62	8.00	3.35

% Error	Confidence Levels (%)		
	90	95	99
	Sample Size		
50	5	7	13
30	15	21	35
20	30	46	80
10	130	200	300
5	550	700	>1000

Table 4						
Moment Magnitude						
Empirical V/H Ratio Weights						
AEF (yr <sup>-1</sup> )	High-Frequency ≥ 5.0 Hz			Low-Frequency ≤ 2.5 Hz		
	Magnitude (M)			Magnitude (M)		
	5.1	7.0	8.0	5.1	7.0	8.0
	Weights			Weights		
10 <sup>-4</sup>	0.37	0.37	0.26	0.20	0.40	0.40
10 <sup>-5</sup>	1.00	0.	0.	0.25	0.25	0.50
10 <sup>-6</sup>	1.00	0.	0.	0.43	0.14	0.43

Empirical V/H Ratio Distances	
Magnitude (M)	Distance (km)
5.1	5
7.0	57
8.0	57

Model V/H Ratio Weights						
AEF (yr <sup>-1</sup> )	High-Frequency ≥ 5.0 Hz			Low-Frequency ≤ 2.5 Hz		
	Distance (km)			Distance (km)		
	28	7	0	28	7	0
	Weights			Weights		
10 <sup>-4</sup>	0.6	0.2	0.2	0.8	0.1	0.1
10 <sup>-5</sup>	0.3	0.7	0.0	0.8	0.1	0.1
10 <sup>-6</sup>	0.1	0.6	0.3	0.4	0.3	0.3

Profile	Weighting		Empirical Relation Weights		Site Condition Weights	
	Empirical	Model	A&S (1997)	C&B (2003)	Soft Rock	Soil
Unit 1	0.2	0.8	0.5	0.5	1.0	0.0

**Notes:**

A&amp;S (1997) = Abrahamson and Silva (1997)

C&amp;B (2003) = Campbell and Bozorgnia (2003)

**FIGURES**

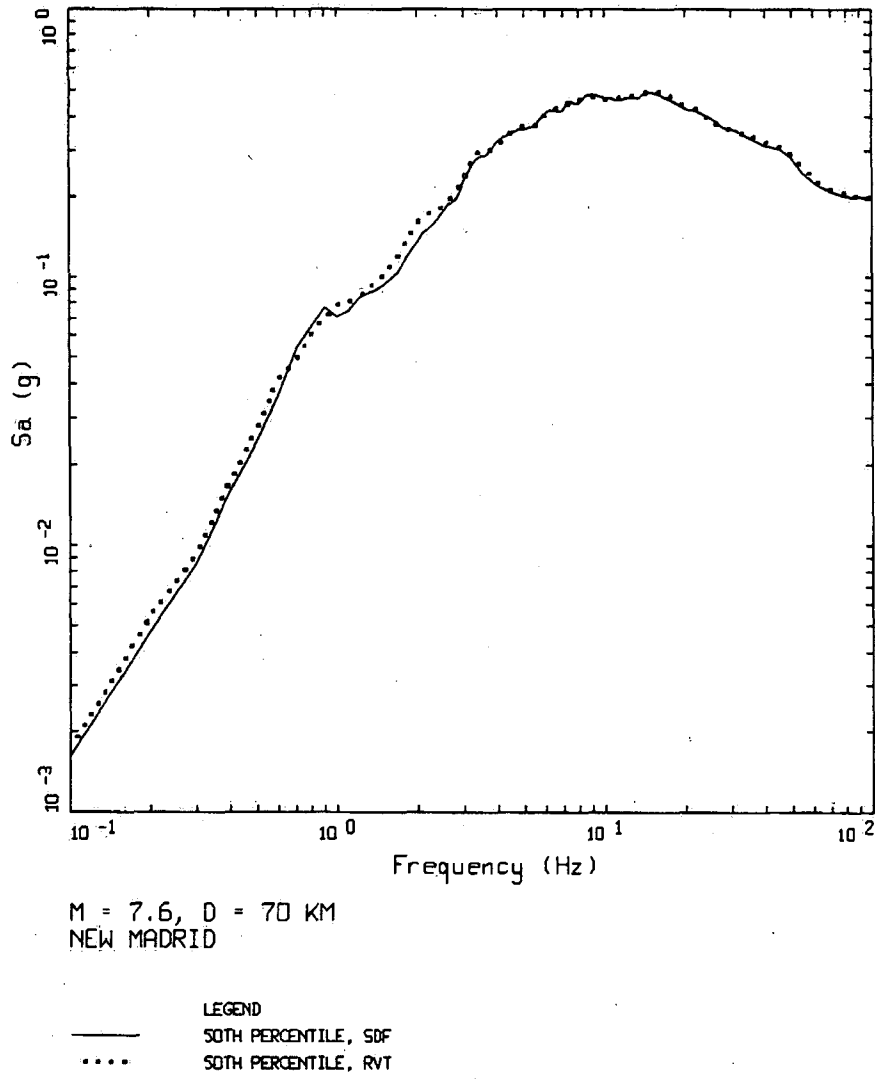
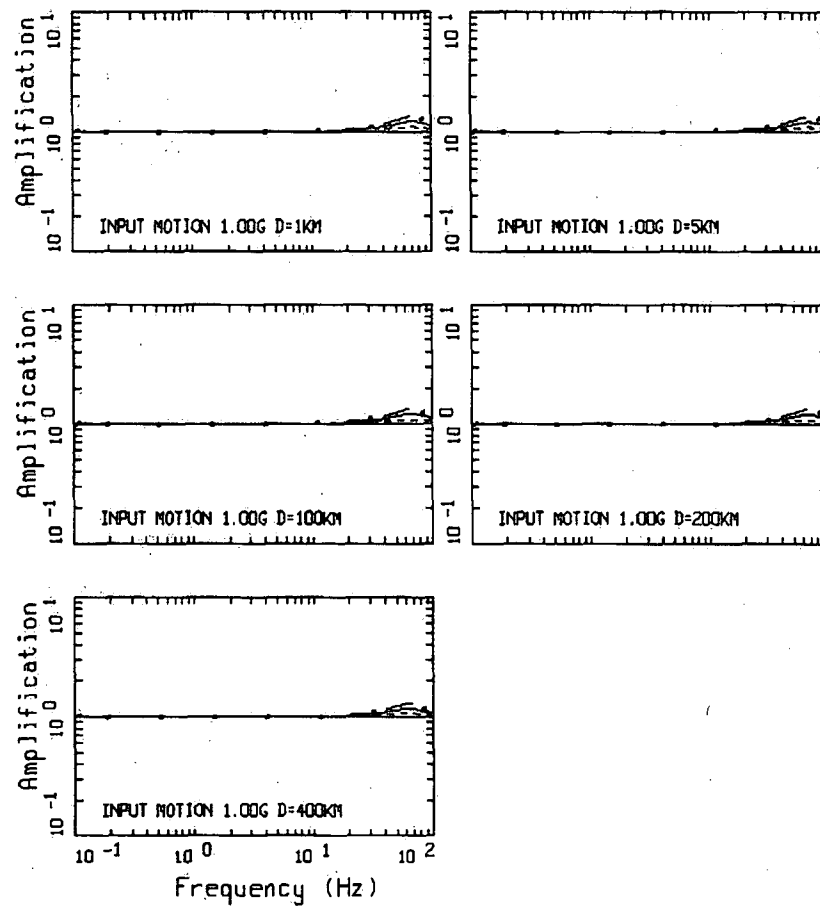


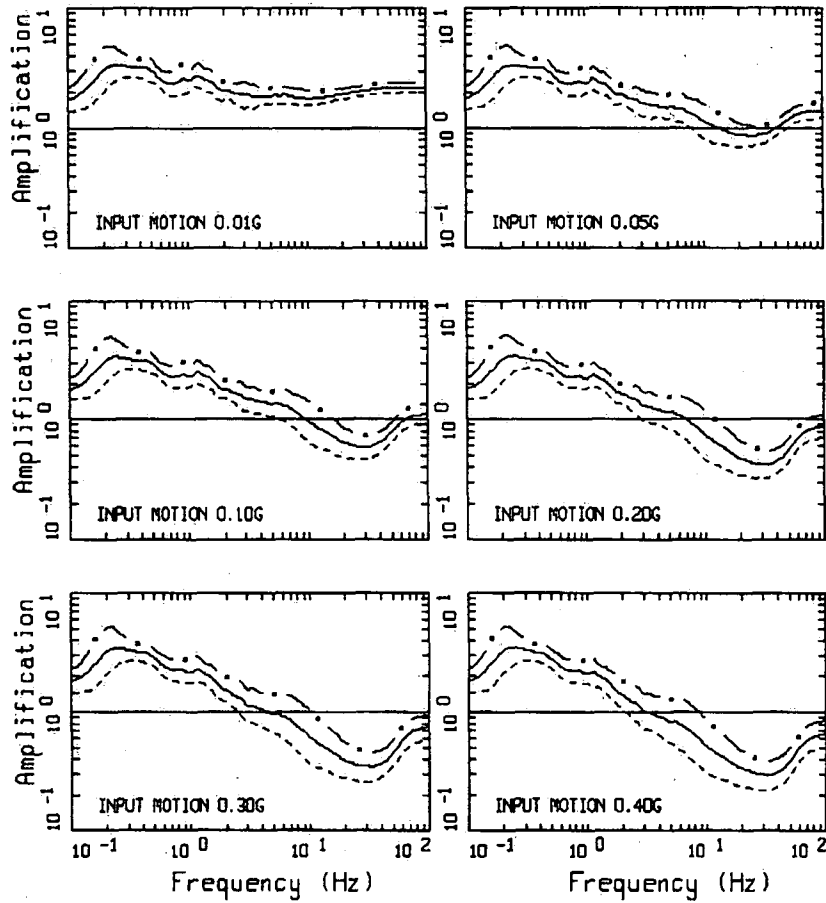
Figure 1. Comparison of median RVT and SDF (computed from acceleration time histories) 5% damped response spectra. Medians computed over 30 realizations.





AMPLIFICATION(H), PROFILE A1

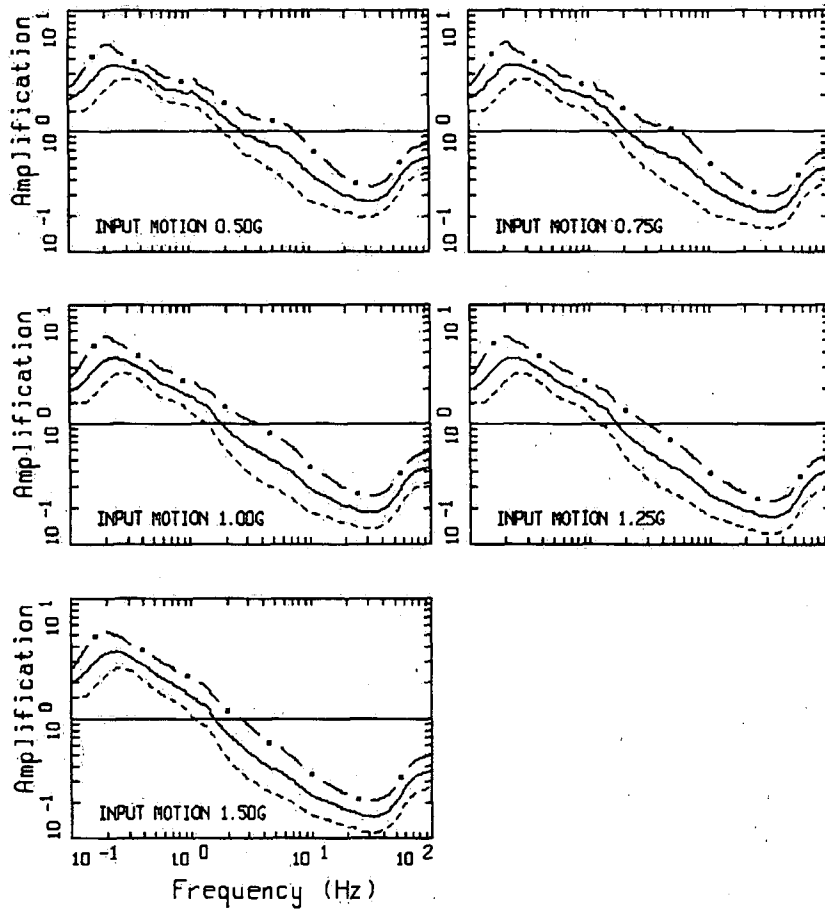
Figure 2. Lee Nuclear Station Unit 1 amplification factors (5% damping) at a suite of source distances. Mean properties: 20 ft concrete with a shear-wave velocity of 7,500 ft/sec over hard rock ( $V_s = 9,300$  ft/sec). Due to the stiffness of the concrete, linear site response analyses were performed. Although M 5.1 was used, based on high frequency deaggregations, response is independent of M due to linearity of the concrete under transient loading (Duke Energy Carolinas, LLC, 2007).



AMPLIFICATION, M = 7.00, 1 CORNER

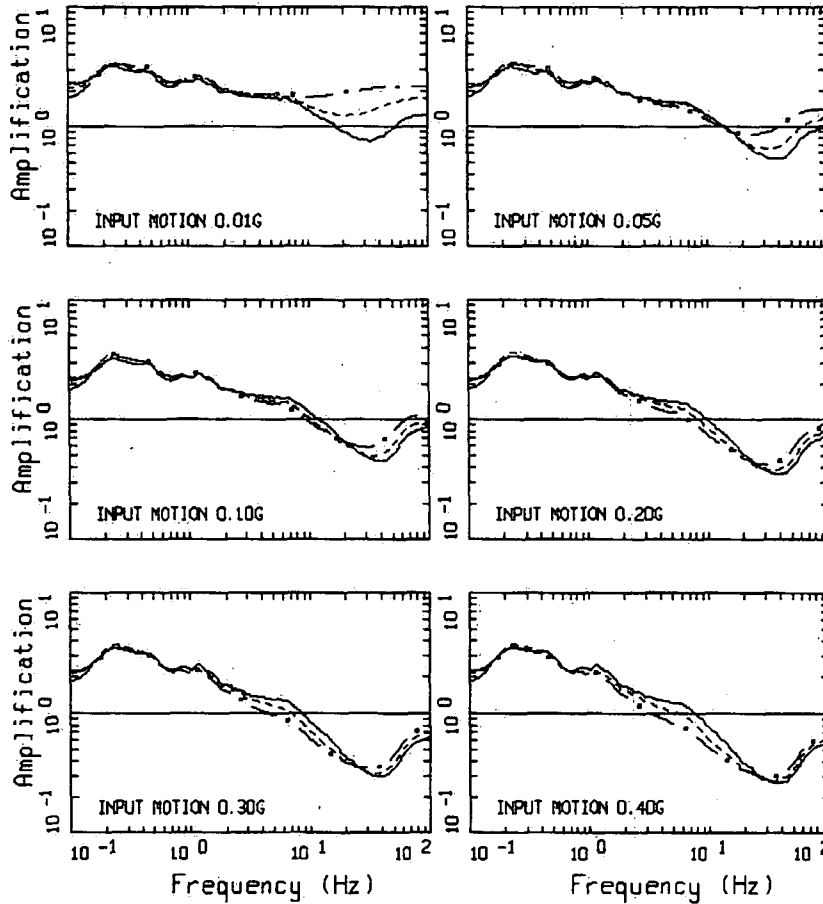
PAGE 1 OF 2

Figure 3. Example of median and  $\pm 1$  sigma estimates of amplification factors computed for deep a soil site in the CENA. Hard rock reference expected peak acceleration ranges from 0.01g to 1.50g. Distances were adjusted to obtain target (input) median peak acceleration values. Single-corner point-source magnitude is 7.0.



AMPLIFICATION, M = 7.00, 1 CORNER  
PAGE 2 OF 2

Figure 3 (cont.)

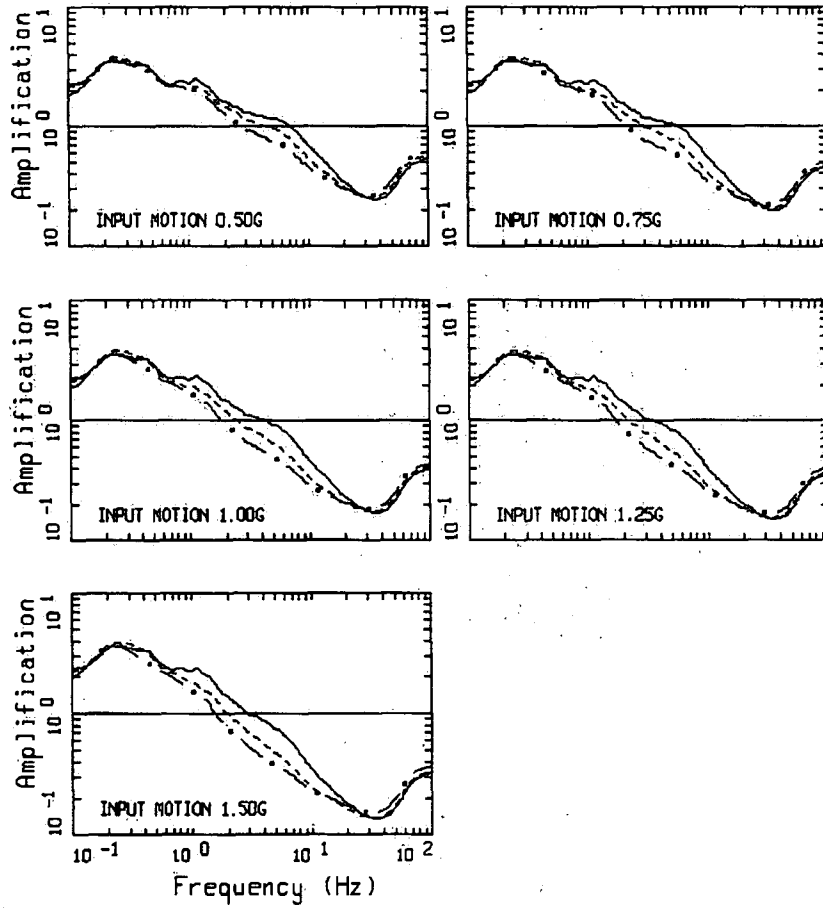


AMPLIFICATION

PAGE 1 OF 2

- LEGEND
- M = 5.0, 1 CORNER
  - - - M = 6.0, 1 CORNER
  - · - M = 7.0, 1 CORNER
  - UNITY LINE

Figure 4. Test case illustrating the effect of magnitude on median amplification factors computed for a deep soil site in the CENA. Distances were adjusted to obtain the target hard rock (input) median peak acceleration values. Plotted versus structural frequency.

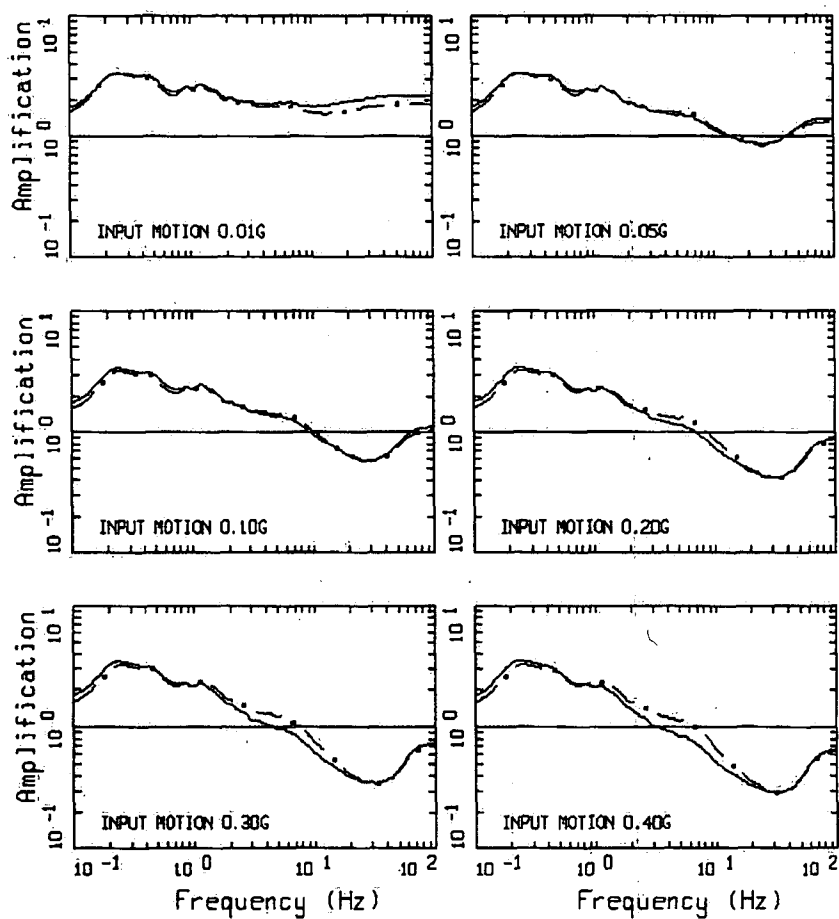


AMPLIFICATION

PAGE 2 OF 2

- LEGEND
- M = 5.0, 1 CORNER
  - - - M = 6.0, 1 CORNER
  - · - M = 7.0, 1 CORNER
  - UNITY LINE

Figure 4 (cont.)

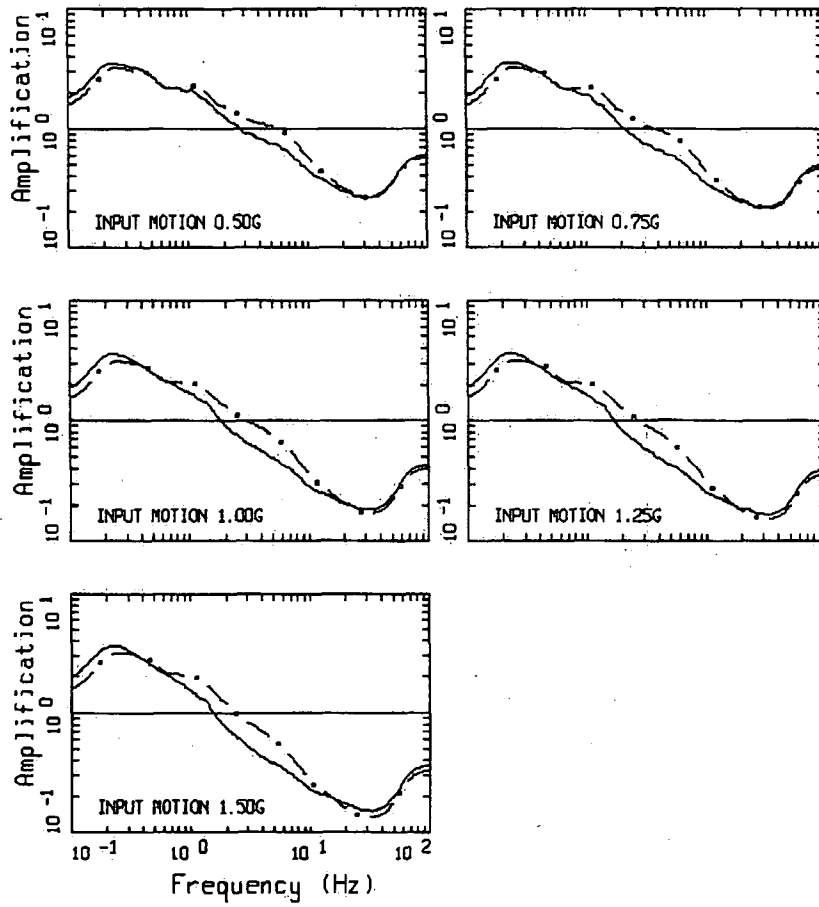


AMPLIFICATION

PAGE 1 OF 2

- LEGEND
- M = 7.0, 1 CORNER
  - - - M = 7.0, 2 CORNER
  - UNITY LINE

Figure 5. Test case illustrating the effect of single-verses double-corner source spectra on median amplification factors computed for a deep soil site in the CENA. Distances were adjusted to obtain the target hard rock (input) median peak acceleration values. Plotted versus structural frequency.

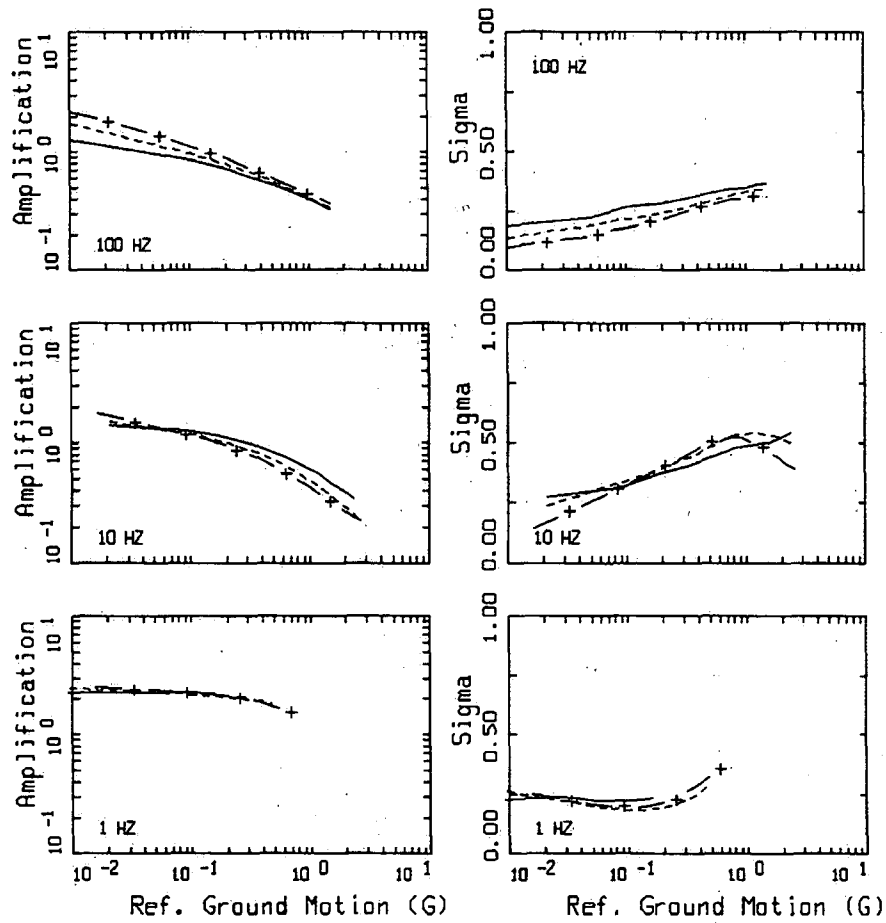


AMPLIFICATION

PAGE 2 OF 2

LEGEND  
— M = 7.0, 1 CORNER  
- - - M = 7.0, 2 CORNER  
— UNITY LINE

Figure 5 (cont.)

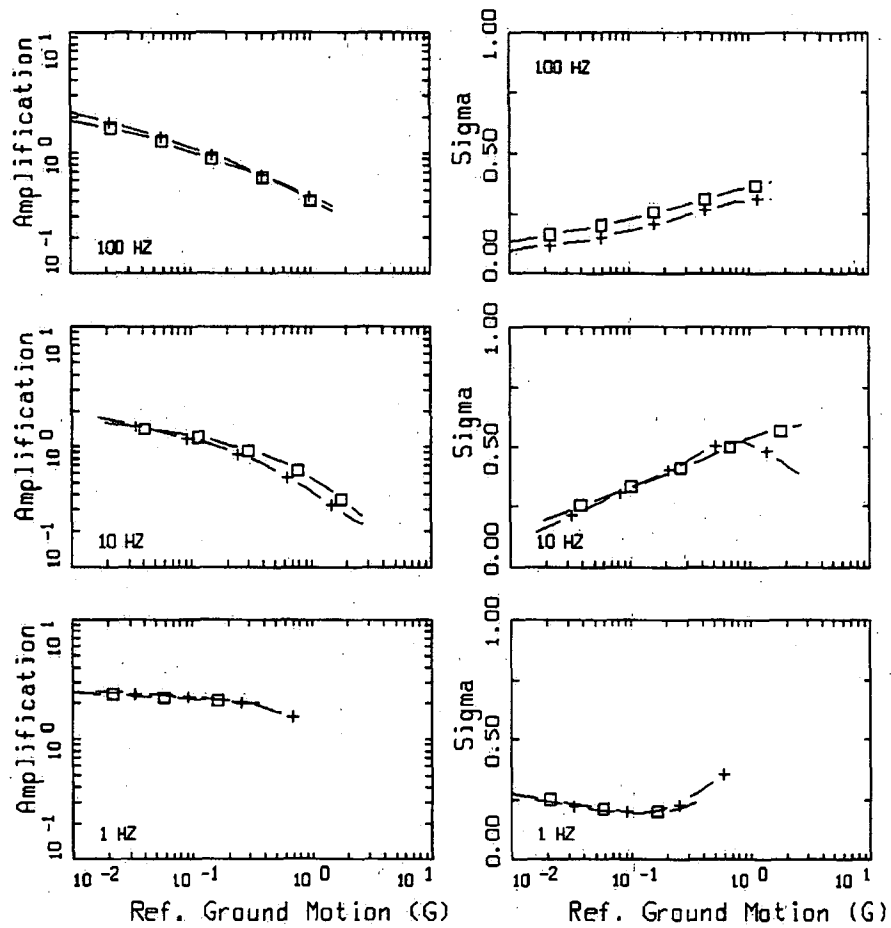


MEDIAN AMPLIFICATION AND SIGMA

- LEGEND
- MS.D, 1 CORNER
  - - - MS.D, 1 CORNER
  - + - M7.D, 1 CORNER

Figure 6. Test case illustrating the effect of magnitude on median amplification factors and sigma values ( $\sigma_{in}$ ) computed for a deep soil site in the CENA. Plotted versus reference site ground motion (5% damped  $S_a$ ) at three structural frequencies.

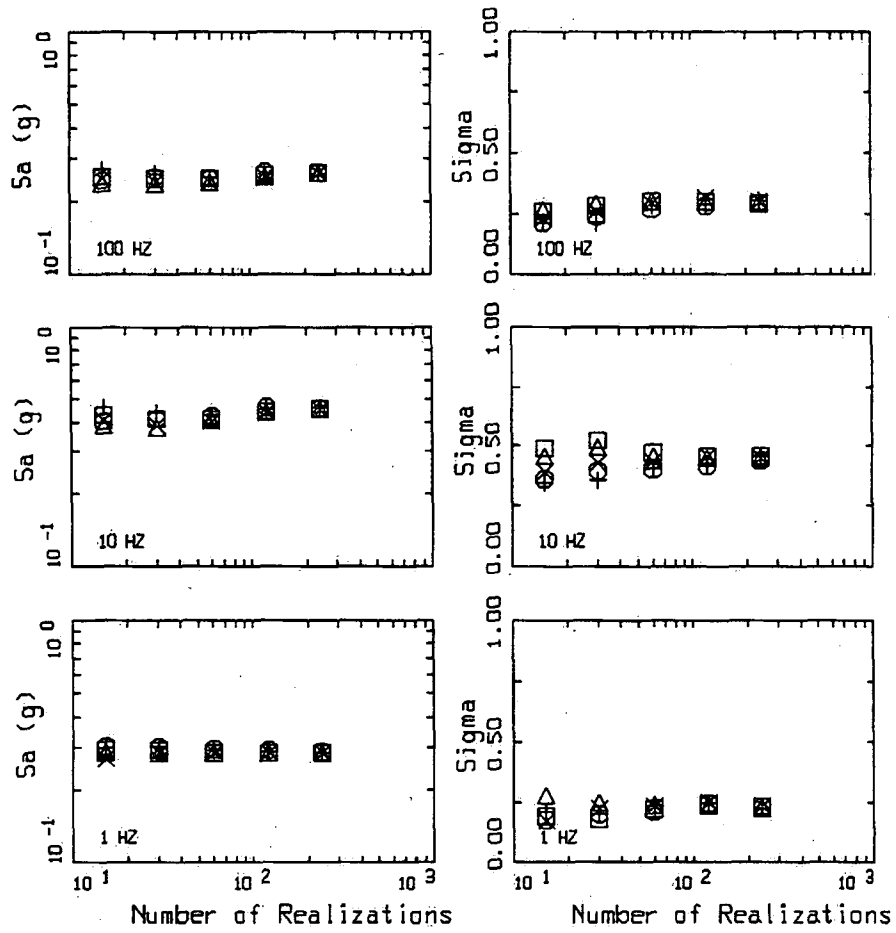




MEDIAN AMPLIFICATION AND SIGMA

LEGEND  
 — + — M7.0, 1 CORNER  
 — o — M7.0, 2 CORNER

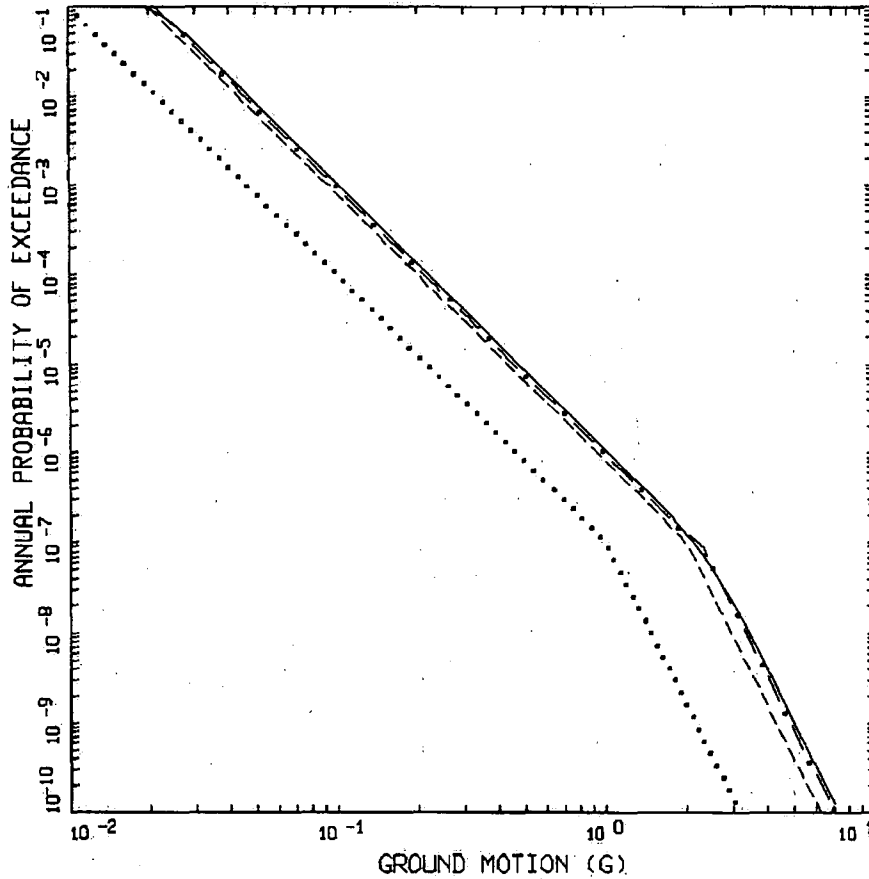
Figure 7. Test case illustrating the effect of single-verses double-corner source spectra on median amplification factors and sigma values ( $\sigma_{in}$ ) computed for a deep soil site in the CENA. Plotted verses reference site ground motion (5% damped  $S_a$ ) at three structural frequencies.



SPECTRAL ACCELERATION AND SIGMA

LEGEND	
□ ··· □	S1
X ··· X	S2
△ ··· △	S3
○ ··· ○	S4
+ ··· +	S5
□ ··· □	
X ··· X	
·	

Figure 8. Median and sigma estimates computed for numbers of realizations from 15 to 240 using five different random seeds for a deep soil site in the CENA.

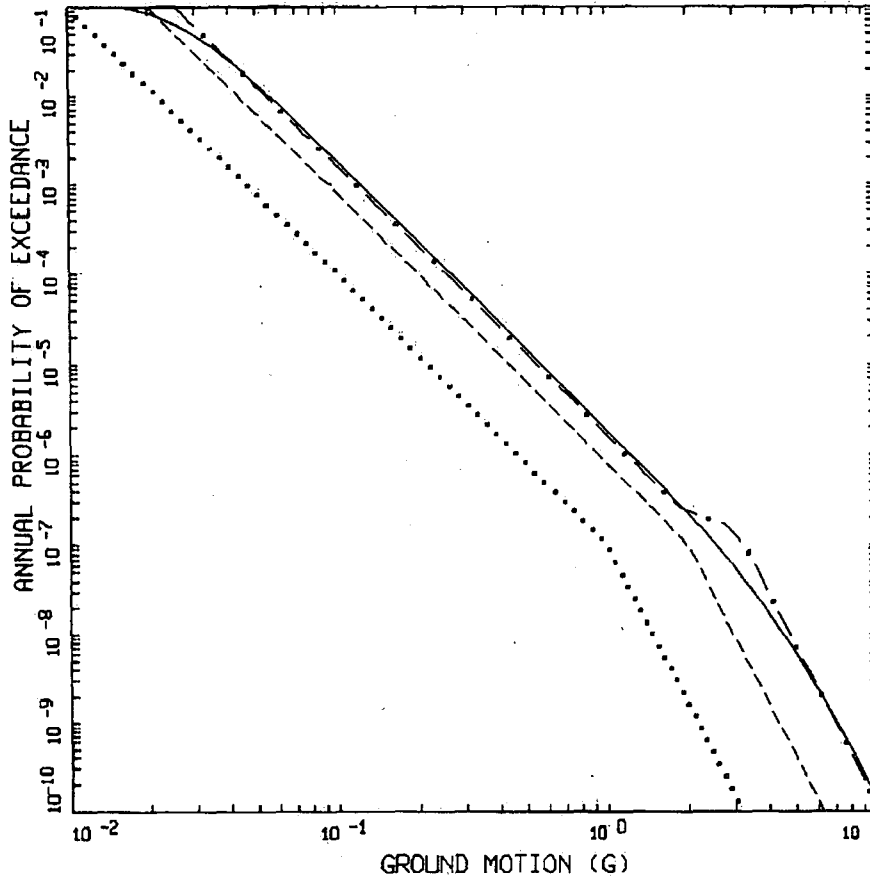


TEST EXAMPLE  
AMP=2.0, SIGMA AMP=0.20

LEGEND  
 ..... INPUT ROCK HAZARD CURVE, SLOPES=3,6  
 - - - - INPUT ROCK HAZARD CURVE MULTIPLIED BY AMP=2.0  
 - . - . OUTPUT SOIL HAZARD CURVE: APPROACH 3 APPROXIMATE  
 \_\_\_\_\_ OUTPUT SOIL HAZARD CURVE: APPROACH 3 FULL INTEGRATION

Figure 9. Test case illustrating Approach 3 using a simple bilinear reference site hazard curve (dotted line, slope = 3, 6). Median amplification factor is 2.0,  $\sigma_n = 0.2$ . Dashed line, reference hazard times median amplification, very close to Approach 2

which uses mean amplification (mean = median  $e^{\frac{\sigma^2}{2}}$ ). Dashed-dot line represents approximate Approach 3 (Equation 7), solid line is full integration Approach 3 (Equation 5). Note the impact of the reference hazard curve slope on the difference between Approaches 2 and 3.

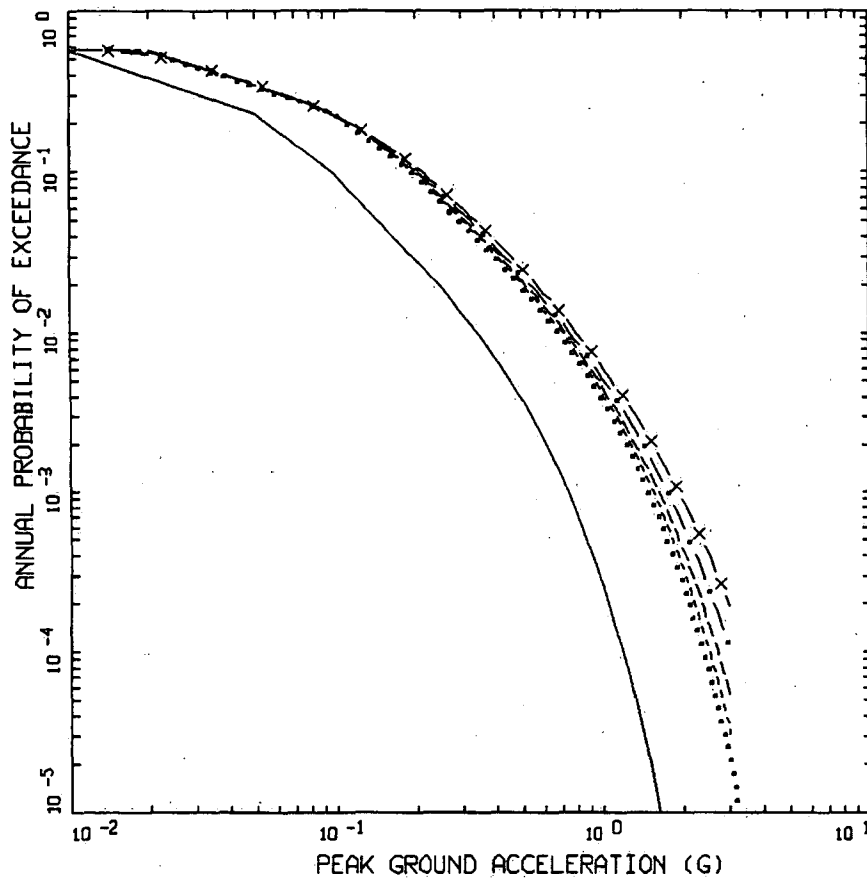


TEST EXAMPLE  
 AMP=2.0, SIGMA AMP=0.40

- LEGEND
- ..... INPUT ROCK HAZARD CURVE, SLOPES=3,6
  - INPUT ROCK HAZARD CURVE MULTIPLIED BY AMP=2.0
  - . - . - . OUTPUT SOIL HAZARD CURVE: APPROACH 3 APPROXIMATE
  - OUTPUT SOIL HAZARD CURVE: APPROACH 3 FULL INTEGRATION

Figure 10. Test case illustrating Approach 3 using a simple bilinear reference site hazard curve (dotted line, slope = 3, 6). Median amplification factor is 2.0,  $\sigma_m = 0.4$ . Dashed line, reference hazard times median amplification, very close to Approach 2

which uses mean amplification (mean = median  $e^{\frac{\sigma^2}{2}}$ ). Dashed-dot line represents approximate Approach 3 (Equation 7), solid line is full integration Approach 3 (Equation 5). Note the impact of the reference hazard curve slope on the difference between Approaches 2 and 3.

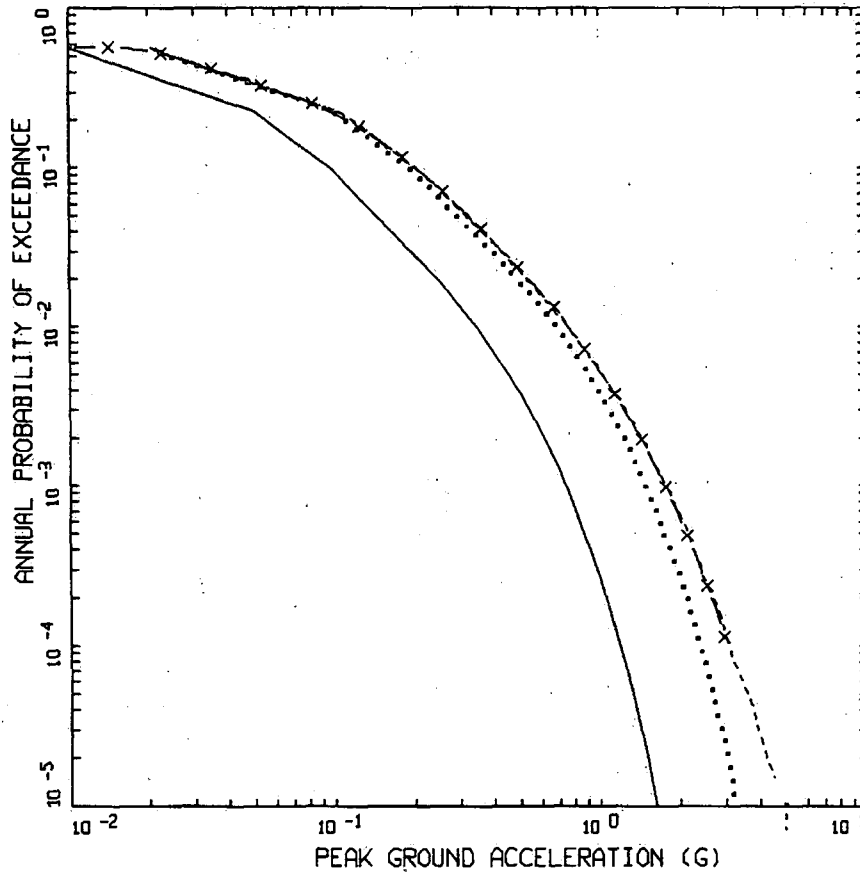


TEST EXAMPLE: PGA HAZARD CURVE  
AMP FACTOR = 2.0

- LEGEND
- INPUT HAZARD CURVE
  - ..... INPUT HAZARD CURVE SCALED BY AMP=2.0
  - APPROACH 3 FULL INTEGRATION: SIGMA = 0.10
  - - - - - APPROACH 3 FULL INTEGRATION: SIGMA = 0.20
  - . - . - APPROACH 3 FULL INTEGRATION: SIGMA = 0.30
  - X - APPROACH 3 FULL INTEGRATION: SIGMA = 0.40

Figure 11. Test case illustrating Approach 3 using a realistic (WNA) reference site hazard curve (solid line). Median amplification factor is 2.0,  $\sigma_{in} = 0.1, 0.2, 0.3, 0.4$ . Dotted line, reference hazard times median amplification, very close to Approach 2

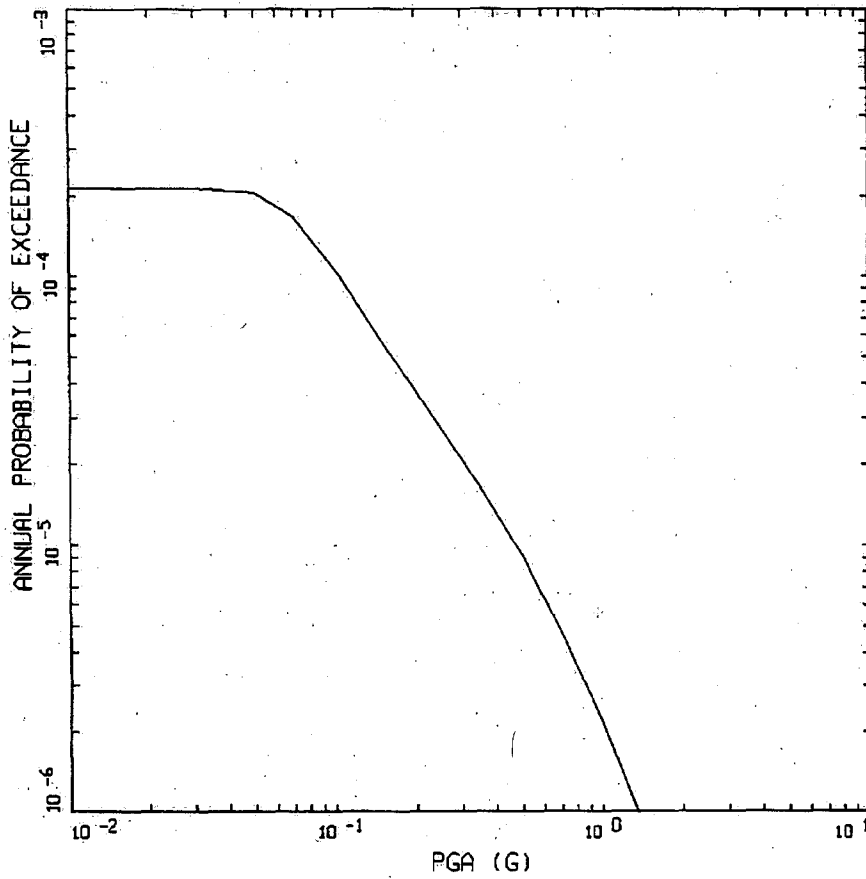
which uses mean amplification (mean = median  $e^{\frac{\sigma^2}{2}}$ ). Note the impact of the reference hazard curve change in slope on the differences between Approaches 2 and 3 (full integration).



TEST EXAMPLE: PGA HAZARD CURVE  
AMP FACTOR = 2.0, SIGMA=0.30

LEGEND  
 ——— INPUT HAZARD CURVE  
 ..... INPUT HAZARD CURVE SCALED BY AMP=2.0  
 - - - - APPROACH 3 APPROXIMATE: SIGMA = 0.30  
 — x — APPROACH 3 FULL INTEGRATION: SIGMA = 0.30

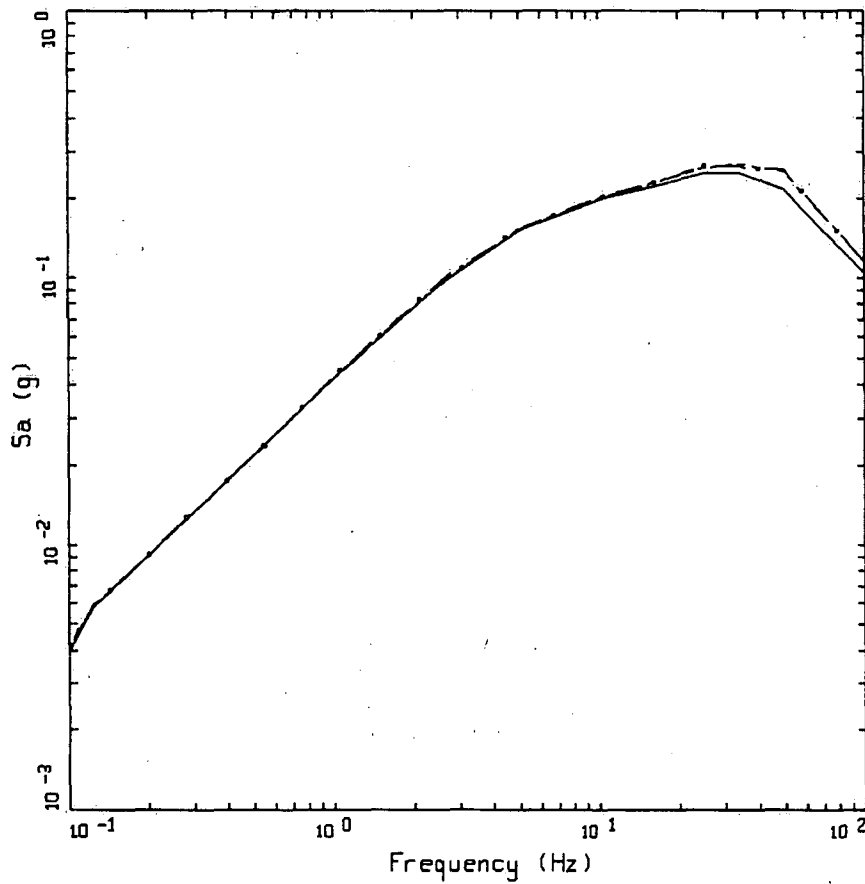
Figure 12. Test case illustrating Approach 3 using a realistic (WNA) reference site hazard curve (solid line). Median amplification factor is 2.0,  $\sigma_n = 0.3$ . Dotted line, reference hazard times median amplification, very close to Approach 2 which uses mean amplification (mean = median  $e^{\frac{\sigma^2}{2}}$ ). Dashed line represents approximate Approach 3 (Equation 7), solid crosses line reflects full integration Approach 3 (Equation 5). Note the impact of the reference hazard curve change in slope on the differences between Approaches 2 and 3 and the breakdown for approximate Approach 3 below AEF of  $2 \times 10^{-4}$ , in this case.



DUKE-LEE: HAZARD CURVE, MEAN  
HARD ROCK, PGA

LEGEND  
— MEAN, PGA

Figure 13. Lee Nuclear Site hard rock horizontal hazard curve for peak acceleration (Duke Energy Carolinas, LLC, 2007).

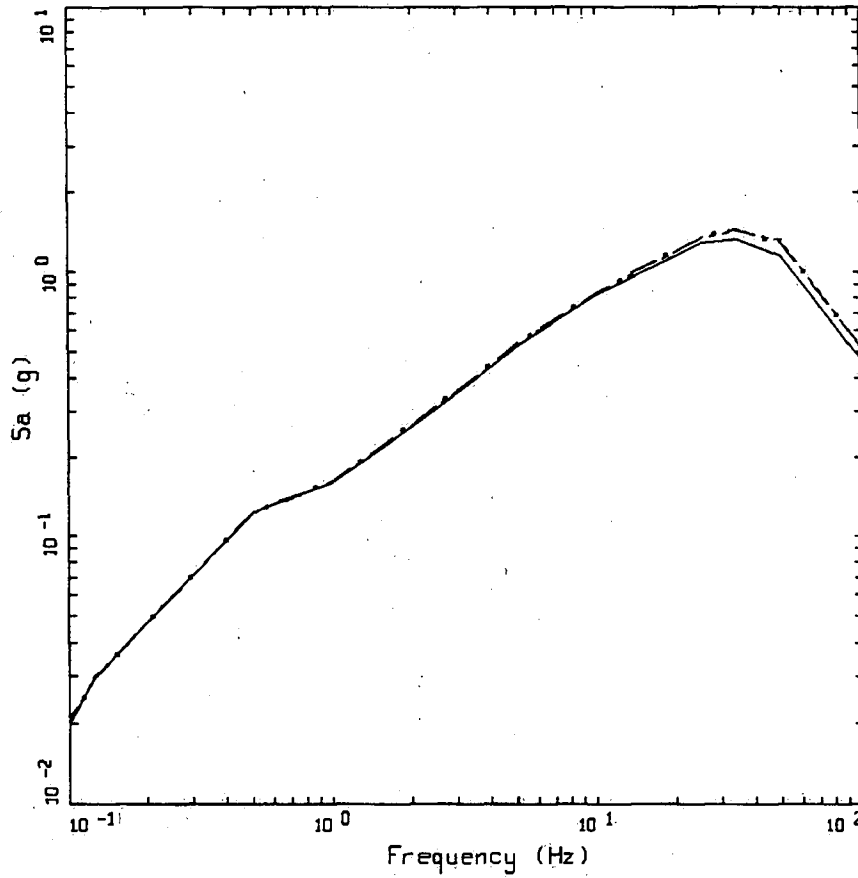


APE =  $1 \times 10^{-4}$  YR<sup>-1</sup>, MEDIAN  
 UHS: HORIZONTAL

- LEGEND
- 5 %, ROCK UHS
  - · - 5 %, PROFILE A1: APPROACH 3 UHS
  - - - 5 %, PROFILE A1: APPROACH 1 UHS

Figure 14. Lee Nuclear Station Unit 1 AEF  $10^{-4}$  horizontal UHS. Hard rock and a comparison between deterministic Approach 1 (or 2, as Approaches 1 and 2 are identical for linear site response) and fully probabilistic Approach 3.





APE =  $1 \times 10^{-5}$  YR<sup>-1</sup>, MEDIAN  
 UHS: HORIZONTAL

- LEGEND
- 5 %, ROCK UHS
  - 5 %, PROFILE A1: APPROACH 3 UHS
  - - - 5 %, PROFILE A1: APPROACH 1 UHS

Figure 15. Lee Nuclear Station Unit 1 AEF  $10^{-5}$  horizontal UHS. Hard rock and a comparison between deterministic Approach 1 (or 2, as Approaches 1 and 2 are identical for linear site response) and fully probabilistic Approach 3.

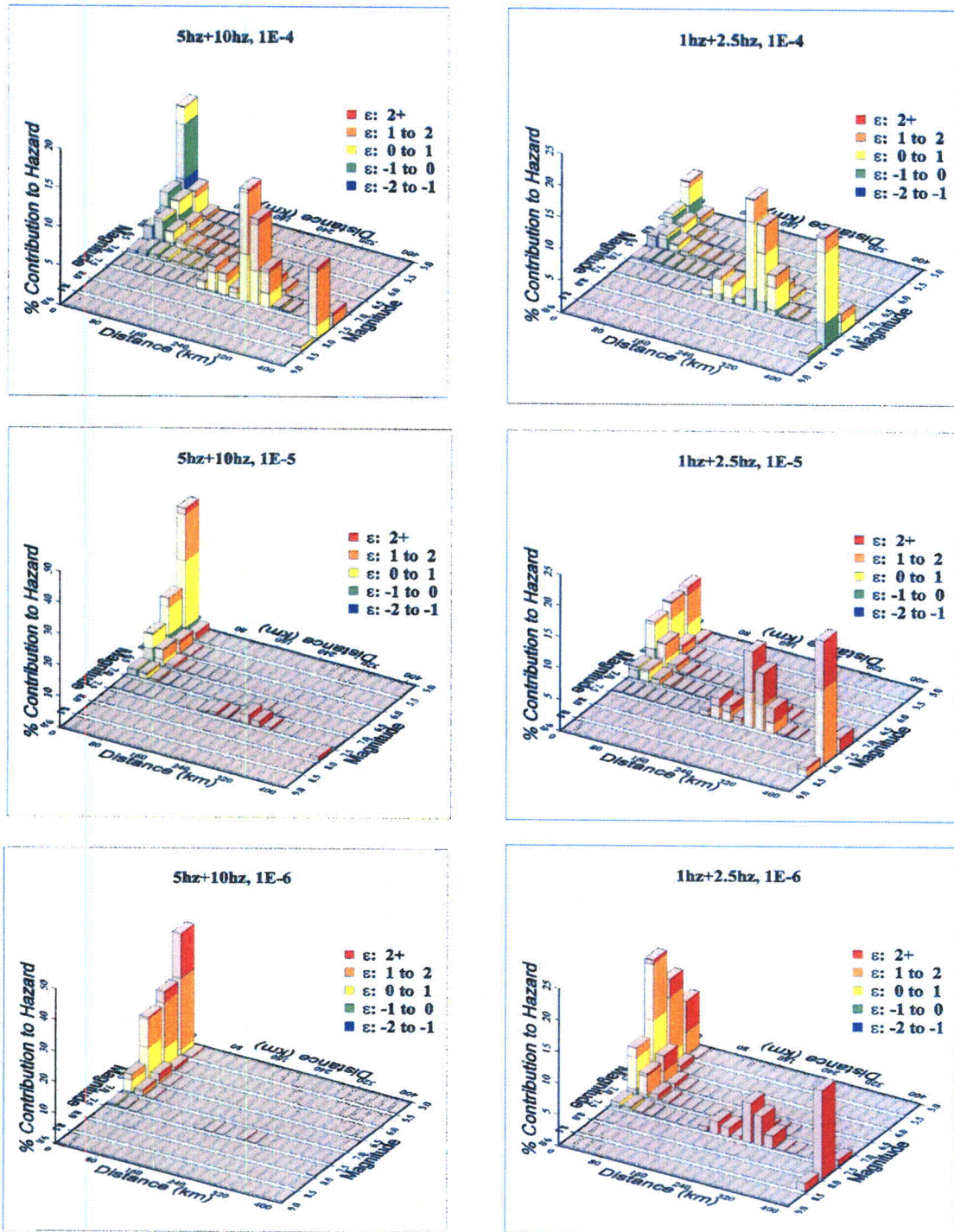
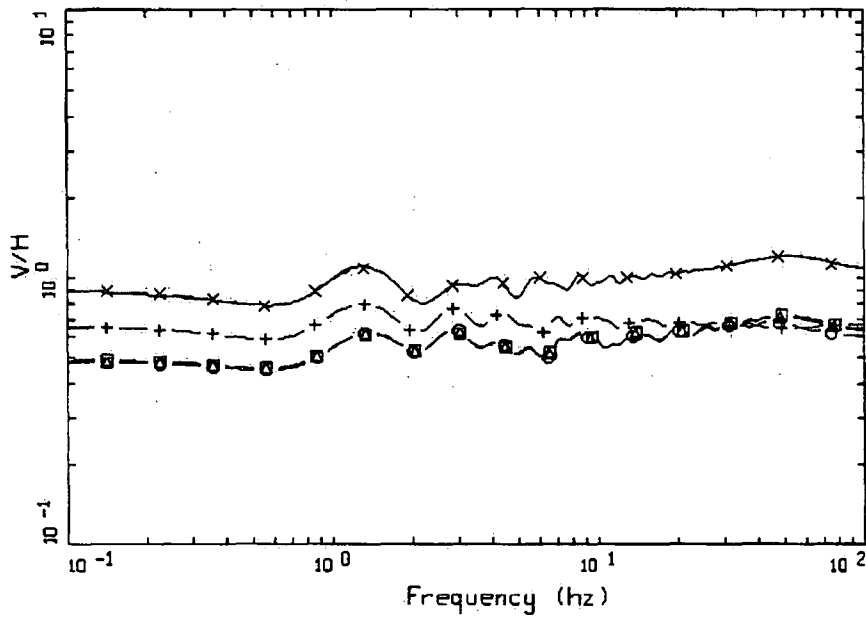


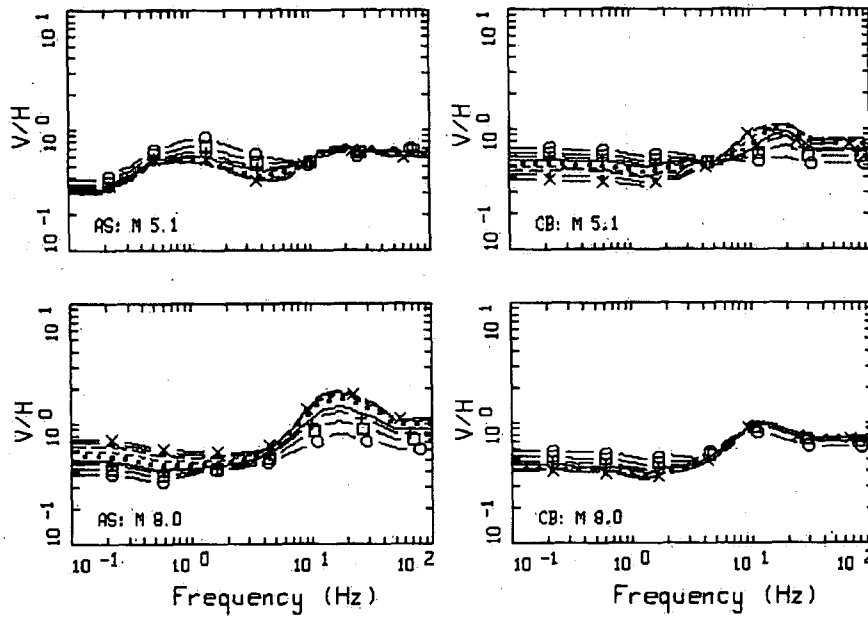
Figure 16. High-frequency ( $\geq 5$  Hz) and low-frequency ( $\leq 2.5$  Hz) hard rock hazard deaggregation for the Lee Nuclear Site (Duke Energy Carolinas, LLC, 2007).



### V/H RATIOS UNIT 1

LEGEND	
—○—	S0TH PERCENTILE, D = 80 KM, 0.01 g
—△—	S0TH PERCENTILE, D = 28 KM, 0.05 g
—□—	S0TH PERCENTILE, D = 16 KM, 0.10 g
—+—	S0TH PERCENTILE, D = 7 KM, 0.20 g
—x—	S0TH PERCENTILE, D = 0 KM, 0.30 g
—	S0TH PERCENTILE, D = 0 KM, 0.50 g

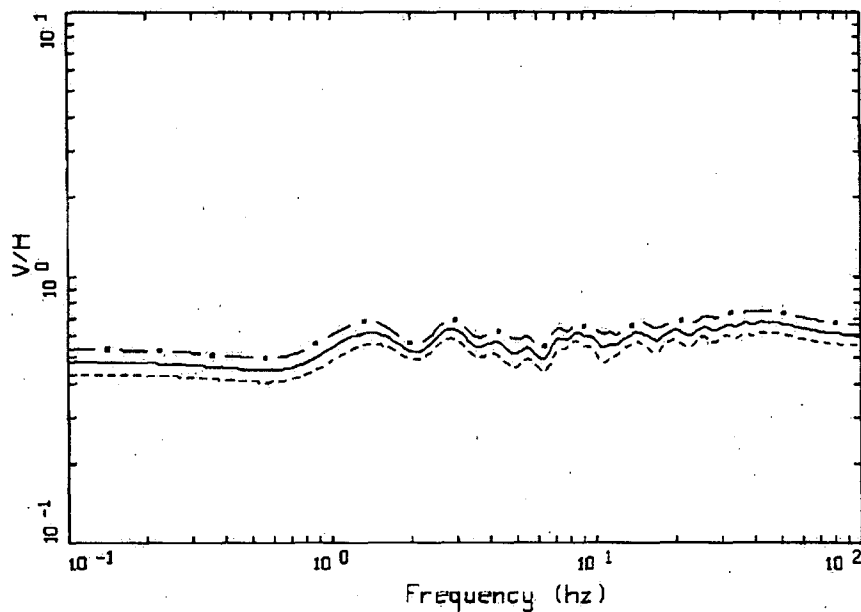
Figure 17. Site-specific median V/H ratios computed for the Lee Nuclear Station Unit 1 for M 5.1 at a suite of distances. Due to profile stiffness linear analyses were performed resulting in magnitude independent V/H ratios (Duke Energy Carolinas, LLC, 2007).



EMPIRICAL V/H RATIOS FOR SOFT ROCK

LEGEND	
—○—	DISTANCE = 57 KM
—□—	DISTANCE = 31 KM
—+—	DISTANCE = 19 KM
—	DISTANCE = 14 KM
.....	DISTANCE = 8 KM
-----	DISTANCE = 5 KM
-----	DISTANCE = 3 KM
-----	DISTANCE = 2 KM
—x—	DISTANCE = 1 KM

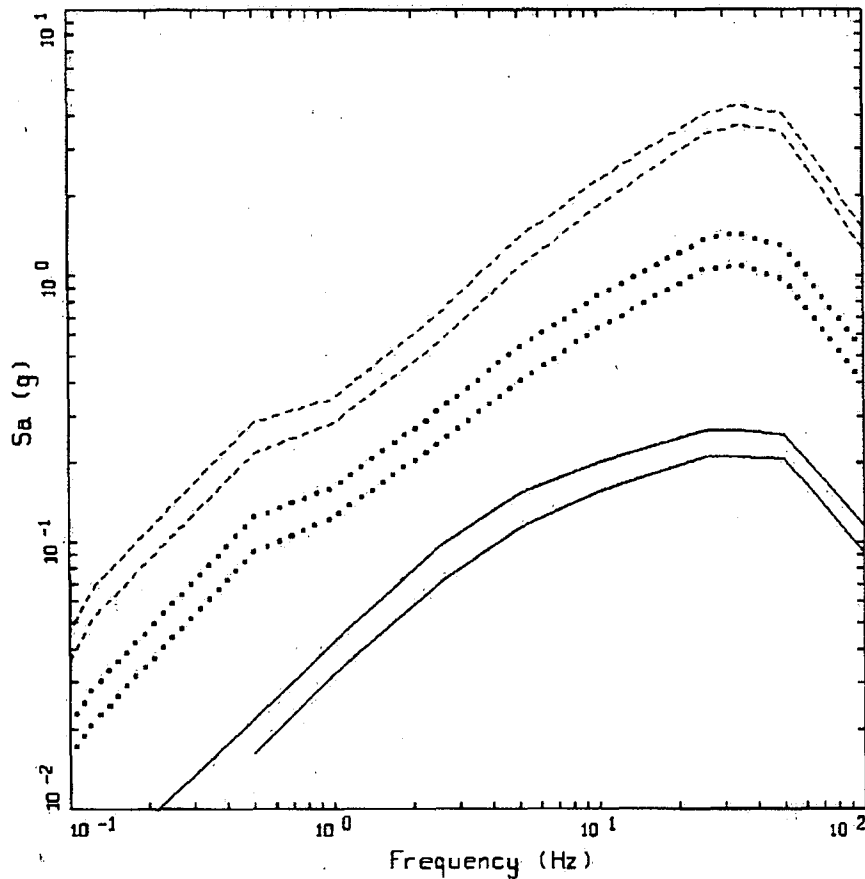
Figure 18. Empirical WNA soft rock median V/H ratios: AS, Abrahamson and Silva, 1997; CB, Campbell and Bozorgnia, 2003 computed for M 5.1 and M 8.0 at a suite of distances.



V/H RATIOS  
UNIT 1

- LEGEND
- 84TH PERCENTILE, D = 80 KM
  - 50TH PERCENTILE, D = 80 KM, 0.01 g
  - ... 16TH PERCENTILE, D = 80 KM

Figure 19. Site-specific median and  $\pm 1$  sigma V/H ratios computed for the Lee Nuclear Station Unit 1 for M 5.1 at a distances of 80 km. Due to profile stiffness linear analyses were performed resulting in magnitude independent V/H ratios. Sigma reflects aleatory variability in shear- and compressional-wave velocities and depth to basement material and across the site.



PROFILE A1  
UHS: HORIZONTAL AND VERTICAL

- LEGEND
- 5 %, HORIZONTAL UHS, MEAN,  $1 \times 10^{-6}$  AEP
  - 5 %, VERTICAL UHS, MEAN,  $1 \times 10^{-6}$  AEP
  - ..... 5 %, HORIZONTAL UHS, MEAN,  $1 \times 10^{-5}$  AEP
  - ..... 5 %, VERTICAL UHS, MEAN,  $1 \times 10^{-5}$  AEP
  - 5 %, HORIZONTAL UHS, MEAN,  $1 \times 10^{-4}$  AEP
  - 5 %, VERTICAL UHS, MEAN,  $1 \times 10^{-4}$  AEP

Figure 20. Horizontal and vertical component UHS at annual exceedance probabilities  $10^{-4}$ ,  $10^{-5}$ ,  $10^{-6}$   $\text{yr}^{-1}$ : Lee Nuclear Station Unit 1 (Duke Energy Carolinas, LLC, 2007).